VYSOKÉ UČENÍ TECHNICKÉ V BRNĚ

BRNO UNIVERSITY OF TECHNOLOGY

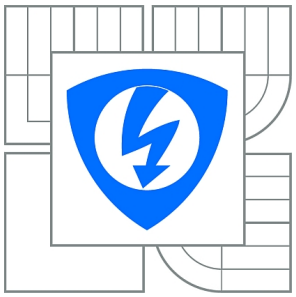

FAKULTA ELEKTROTECHNIKY A KOMUNIKAČNÍCH TECHNOLOGIÍ

ÚSTAV VÝKONOVÉ ELEKTROTECHNIKY A ELEKTRONIKY

FACULTY OF ELECTRICAL ENGINEERING AND COMMUNICATION

DEPARTMENT OF POWER ELECTRICAL AND ELECTRONIC ENGINEERING

ALGORITHMS FOR THE CONTROL OF THE INDUCTION MOTOR

ALGORITMY PRO ŘÍZENÍ ASYNCHRONNÍHO MOTORU

DIPLOMOVÁ PRÁCE

MASTER'S THESIS

AUTOR PRÁCE — Bc. VLADIMÍR HUNDÁK

AUTHOR

VEDOUCÍ PRÁCE — doc. Dr. Ing. MIROSLAV PATOČKA

SUPERVISOR

BRNO 2014

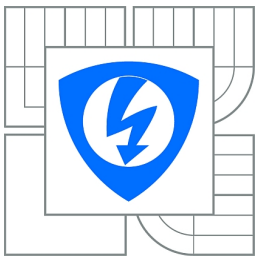

VYSOKÉ UČENÍ TECHNICKÉ V BRNĚ

Fakulta elektrotechniky a komunikačních technologií

Ústav výkonové elektrotechniky a elektroniky

Diplomová práce

magisterský navazující studijní obor
Silnoproudá elektrotechnika a výkonová elektronika

Student:	Bc. Vladimír Hundák	***ID:***	151303
Ročník:	2	***Akademický rok:***	2013/2014

NÁZEV TÉMATU:

Algoritmy pro řízení asynchronního motoru

POKYNY PRO VYPRACOVÁNÍ:

1. Seznamte se s principy vektorového řízení asynchronního motoru. Definujte a matematicky popište základní typy vektorového řízení.
2. Vytvořte matematický model asynchronního motoru 2,2kW, model trojfázového střídače a model trojfázového PWM modulátoru v prostředí Matlab-Simulink.
3. V prostředí Matlab-Simulink realizujte základní známé typy řídicích algoritmů vektorového řízení. Realizujte rovněž řídicí algoritmus nového typu, jehož autorem je vedoucí diplomové práce. Vlastnosti všech algoritmů ověřte simulací.

DOPORUČENÁ LITERATURA:

[1] Patočka M.: Magnetické jevy a obvody. VUTIUM, Brno, 2011.
[2] Patočka M.: Vybrané statě z výkonové elektroniky, sv.1. Skriptum, FEKT, VUT Brno.
[3] Patočka M.: Vybrané statě z výkonové elektroniky, sv.2. Skriptum, FEKT, VUT Brno.

Termín zadání:	27.9.2013	***Termín odevzdání:***	28.5.2014

Vedoucí práce: doc. Dr. Ing. Miroslav Patočka
Konzultanti diplomové práce:

Ing. Ondřej Vítek, Ph.D.
Předseda oborové rady

UPOZORNĚNÍ:

BRNO, 2014

Abstract

The main aim of this thesis is to perform simulations of various control algorithms of the induction machine and mutual comparison of their properties. It also deals with equivalent circuit configuration variants using T-network, Γ-network and Ί-network. The work includes both theoretical analysis, as well as simulations of individual control types. Detailed guide for realization of each simulation is also included. In total, three simulations will be performed – simulation of rotor oriented vector control, stator oriented vector control and simulation of so-called natural control. It is completely new type of control whose author is supervisor of this thesis. Its simulation was the very first attempt of functional realization of this type of control.

Abstrakt

Hlavným cieľom tejto práce je vytvorenie simulácií rôznych algoritmov riadenia asynchrónneho motora a vzájomné porovnanie ich vlastností. Zaoberá sa taktiež možnosťami konfigurácie náhradného zapojenia na T-článok, Γ-článok a Ί -článok. Obsahuje jednak teoretický rozbor, a taktiež aj simulácie jednotlivých spôsobov riadenia spolu s podrobným návodom na ich realizáciu. Celkovo budú vykonané 3 simulácie – simulácia vektorového riadenia s orientáciou na rotorový tok, vektorového riadenia s orientáciou na statorový tok a simulácia takzvaného prirodzeného riadenia. Ide o úplne nový typ riadenia, ktorého autorom je vedúci tejto diplomovej práce. Jeho simulácia bola vôbec prvým pokusom o funkčnú realizáciu tohto typu riadenia.

Keywords

induction machine, vector control, equivalent circuit, block diagram, simulation, mathematical model, pulse width modulation, Simulink

Klíčová slova

asynchronní motor, vektorové řízení, náhradní zapojení, blokové schéma, simulace, matematický model, pulzně šířková modulace, Simulink

Bibliografická citace

HUNDÁK, V. *Algorithms for the Control of the Induction Motor*. Brno: Vysoké učení technické v Brně, Fakulta elektrotechniky a komunikačních technologií, 2014. 66 s. Vedoucí diplomové práce doc. Dr. Ing. Miroslav Patočka.

Prohlášení

Prohlašuji, že svou diplomovou práci na téma Algorithms for the Control of the Induction Motor jsem vypracoval samostatně pod vedením vedoucího semestrální práce a s použitím odborné literatury a dalších informačních zdrojů, které jsou všechny citovány v práci a uvedeny v seznamu literatury na konci práce.

Jako autor uvedené semestrální práce dále prohlašuji, že v souvislosti s vytvořením této semestrální práce jsem neporušil autorská práva třetích osob, zejména jsem nezasáhl nedovoleným způsobem do cizích autorských práv osobnostních a jsem si plně vědom následků porušení ustanovení § 11 a následujících autorského zákona č. 121/2000 Sb., včetně možných trestněprávních důsledků vyplývajících z ustanovení § 152 trestního zákona č. 140/1961 Sb.

V Brně dne 28. 5. 2014 Podpis autora ……..

Poděkování

Děkuji vedoucímu diplomové práce doc. Dr. Ing. Miroslavu Patočkovi za účinnou metodickou, pedagogickou a odbornou pomoc a další cenné rady při zpracování mé semestrální práce.

V Brně dne 28. 5. 2014 Podpis autora ……..

CONTENTS

LIST OF PICTURES

LIST OF SYMBOLS

C	capacitance
f	frequency
f_{PWM}	frequency of PWM carrier signal
F	transfer function
F_{si}	transfer of current sensor
F_{fi}	transfer of frequency inverter
F_S	transfer function of system
G	gain
i	actual value of current
I	current
I_1	stator current
I_{1n}	nominal stator current
I_2	rotor current
I_T	torque-producing component of rotor current
I_μ	magnetizing current
I_σ	reactive component of rotor current
J	moment of inertia
k	coupling factor
K	auxiliary parameter
$K_{I,21,K}$	current transfer at short-circuit state
$K_{V,21,0}$	voltage transfer at no-load state
L	inductance
L_1	stator inductance
L_2	rotor inductance
L_e	equivalent inductance (auxiliary parameter)
L_h	main inductance
L_{h1}	main inductance of stator winding
L_{h2}	main inductance of rotor winding
L_p	parallel inductance

$L_{\sigma 1}$	leakage inductance of stator winding
$L_{\sigma 2}$	leakage inductance of rotor winding
M	mutual inductance, modulation index
p	Laplace operator
p_p	number of pairs of poles
P	power
P_1	power behind resistance R_1 (auxiliary parameter)
P_{mech}	mechanical power
P_n	nominal power
R	resistance, regulator
R_1	resistance of stator winding
R_2	squirrel cage resistance
R_e	equivalent resistance (auxiliary parameter)
R_i	current regulator
R_L	resistive load
R_p	parallel resistance
R_ψ	regulator of magnetic flux
R_ω	speed regulator
s	slip
t	time
t_1	value of room temperature
T_i	torque produced by motor
T_L	mechanical load
v	actual value of voltage
V	voltage
V_1	stator voltage, input voltage
V_{1n}	nominal voltage on stator terminals
V_d	inverter DC bus voltage
V_μ	magnetizing voltage
η	efficiency
σ	arbitrary chosen parameter

τ	time constant
τ_{fi}	time constant of frequency inverter
τ_R	rotor time constant
τ_σ	arbitrary chosen time constant
ϑ	transformation angle, temperature
ψ	magnetic flux
ψ_1	stator magnetic flux
ψ_2	rotor magnetic flux
ψ_w	reference value of magnetic flux
ω	angular velocity
ω_1	angular velocity of stator magnetic field
ω_2	angular velocity of rotor
ω_n	nominal mechanical angular velocity
ω_w	reference value of angular velocity
Ω_m	mechanical angular velocity

INTRODUCTION

Squirrel-cage induction machines have a wide application range in industrial production. This range of use mostly comes from their properties, for example operation reliability, easy maintenance, sturdiness, or reasonable price.

However, in the past there existed a major disadvantage of these machines in difficult speed control. This significant disadvantage could be suppressed thankfully to technological development in the last decades. It enabled decrease in price of frequency inverters, an increase in their reliability and enabled application of modern methods of real-time control, as well. The main task in quality improvement of induction machine drives could be shifted to other fields, such as creation of control algorithms. These algorithms should be able to suppress non-linear properties of induction machines, eventually enable control of drive even without speed sensor.

High accuracy of induction machine drives speed control is enabled with so-called vector control. It simplifies the control of induction motors and makes it closer to the control of DC motor with external excitation, which is much simpler in principle. However, this type of control is not the only used control algorithm. There also exist many other algorithms based on completely different principles, and many new ideas are still being born.

1 EQUIVALENT CIRCUIT CONFIGURATION VARIANTS OF THE INDUCTION MOTOR

This chapter deals with analysis of various equivalent circuit configuration variants of the induction motor, specifically equivalent circuit using T-network, Γ-network and Ί-network. It is an analogy to the analysis of different equivalent circuit configuration variants of transformer, which can be found in literature [1]. Firstly, it is necessary to derive induction machine number of degrees of freedom as a passive two-port network to be able to properly explain the configuration process, described in following chapters.

1.1 Passive two-port network number of degrees of freedom

In general, two-port network is random electric circuit, which can be attached to another electric circuit with two pairs of terminals – two gates. Two-port network is stated as passive, when it contains only passive elements (resistance R, inductance L, capacitance C), thus it does not contain any current or voltage sources. First couple of terminals serves as an input gate, through which energy enters into the network. Similarly, the second gate serves as an output gate.

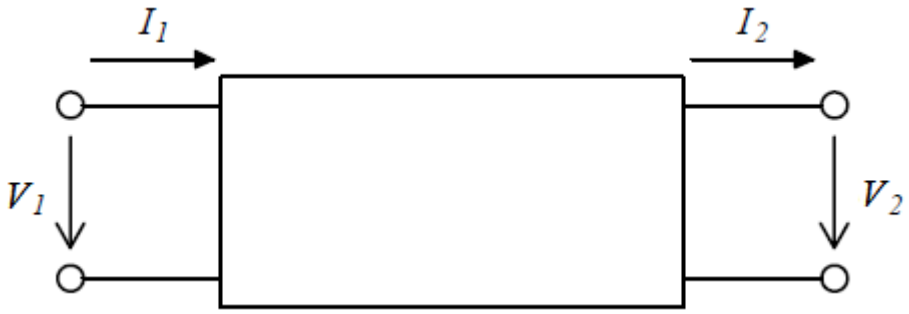

Pic. 1.1-1: Graphic interpretation of two-port network; label of input and output parameters.

Circuit behavior (behavior of external parameters – current and voltage) is analyzed across the network terminals, where the internal connection of this two-port network can be no matter how complicated. Therefore, external behavior can be described using vectors of two voltages and two currents. As a result, it is possible to fully describe properties of two-port network using square matrix with dimensions of 2x2. An equation (1.1-1) where two-port network is described using Z-matrix is given as an example:

$$\begin{bmatrix} V_1 \\ V_2 \end{bmatrix} = \begin{bmatrix} z_{11} & z_{12} \\ z_{21} & z_{22} \end{bmatrix} x \begin{bmatrix} I_1 \\ I_2 \end{bmatrix} \tag{1.1-1}$$

Principle of reciprocity is valid for passive two-port network – equal energy is transferred in both directions, therefore it does not matter which couple of terminals is considered as an input and which one as an output. From that can be derived that matrix of the network must be symmetric across main diagonal, therefore it is valid that $z_{12} = z_{21}$. This statement can be used as a proof that out of four matrix elements only three are different. This proves following statements:

- each passive transmission two-port network has only three degrees of freedom
- it can be always substituted by equivalent three-pole using T-network, eventually Π-network, consisting of three impedances
- all transfer properties of two-port network are fully defined by three independent parameters (for example L_1, L_2, M)

1.2 Direct separation of leakage inductances

The following analysis considers an induction machine as a linear transmission two-port network, where its properties will be used. According to the ideas stated in previous chapter, it is possible to define parameters of an induction machine, using three independent circuit parameters, for example. However, from the well-known equation for mutual inductance of two coils (1.2-1) results that parameters of the quadruplet L_1, L_2, M, k are dependent on each other and therefore one parameter is excessive.

$$M = k\sqrt{L_1.L_2} \tag{1.2-1}$$

In the cases where coupling factor k is close to 1 – for very tight magnetic binding, it is possible to omit k and claim that it equals 1 at the cost of relatively small calculation error. However, for the induction machine the k is approximately equal 0,93 [1]. This would cause significant inaccuracy of the equivalent circuit and of a related mathematical model in the case of omitting this parameter. Therefore, the coupling factor cannot be neglected. Thus, the process of leakage inductances separation will have infinitely many solutions.

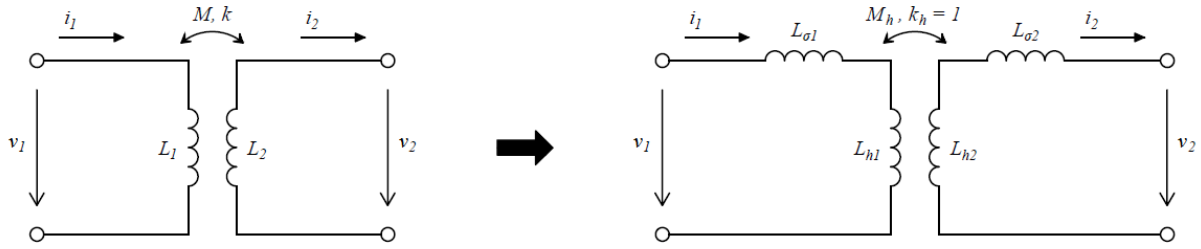

Pic. 1.2-1: Direct separation of induction motor leakage inductances.

Original two-port network contains three degrees of freedom; therefore, final two-port network, created by separation, must only consist of three degrees of freedom, as well. However, in reality, it contains as many as four unknown parameters, specifically two main inductances L_{h1}, L_{h2} and two leakage inductances $L_{\sigma 1}, L_{\sigma 2}$. It means that the process of separation is not clearly defined and so it is necessary to make an arbitrary choice of one parameter and obtain remaining three parameters using this relation.

One possibility of direct separation of leakage inductances is presented in *Pic. 1.2-1*. The inductances L_{h1}, L_{h2} create an ideal transformer where k_h = 1. Using this information, we obtain three searched values of ideal transformer L_{h1}, L_{h2}, M_h, where equation (1.2-2) is valid:

$$M_h = \sqrt{L_{h1}.L_{h2}} \tag{1.2-2}$$

Detailed procedure of separation can be found in literature [1] (chapter 17.5.1, page 354-356). It was necessary, during the separation process, to implement dimensionless arbitrary chosen parameter σ. This parameter represents excessive degree of freedom in order to maintain the free choice possibility out of the infinite number of solutions. The result is represented with an equation system (1.2-3) – (1.2-8).

Following equations were derived to determine the value of leakage inductances:

$$L_{\sigma 1} = L_1 \left(1 - \frac{k}{\sigma}\right) \tag{1.2-3}$$

$$L_{\sigma 2} = L_2 (1 - k\sigma) \tag{1.2-4}$$

Moreover, values of main inductances can be defined as follows:

$$L_{h1} = \frac{k}{\sigma} L_1 \tag{1.2-5}$$

$$L_{h2} = k\sigma L_2 \tag{1.2-6}$$

Equation for calculating mutual inductance can be obtained by substituting equations (1.2-5) and (1.2-6) into equation (1.2-2):

$$M_h = M = k\sqrt{L_1 . L_2} \tag{1.2-7}$$

The function of last equation is to calculate voltage transfer at no-load state, or differently said transfer ratio of separated ideal transformer:

$$K_{h,V,21,0} = \sqrt{\frac{L_{h2}}{L_{h1}}} = \sigma \sqrt{\frac{L_2}{L_1}} \tag{1.2-8}$$

It is possible to recalculate rotor impedances to the stator side by using square of this transfer ratio. Implemented parameter σ can be freely chosen except the zero value. In that case a division by zero would appear during the calculation of L_{h1} and $L_{\sigma 1}$. Therefore, this parameter must be chosen inside the intervals:

$$\sigma \in (-\infty\ ;\ 0) \cup (0\ ;\ +\infty) \tag{1.2-9}$$

However, it is possible that some of the inductances $L_{h1}, L_{h2}, L_{\sigma 1}, L_{\sigma 2}$ gain negative value depending on the chosen value of parameter σ. Although, this solution cannot be realized physically, it is mathematically correct. In the case that we demand physically realizable equivalent circuits it is necessary to choose the value of parameter σ from the interval resulting from the equations (1.2-3) and (1.2-4).

$$k \leq \sigma \leq \frac{1}{k} \tag{1.2-10}$$

The selection of parameter σ fulfilling inequality (1.2-10), except the marginal values, ensures physically realizable equivalent circuit (where all of the inductances $L_{h1}, L_{h2}, L_{\sigma 1}, L_{\sigma 2}$ gain positive value). The selection of parameter σ not fulfilling this inequality defines physically non-realizable but fully valued equivalent circuits (where at least one of the inductances gains negative value). Especially interesting is the choice of parameter σ as one of the inequality marginal values. Following chapters 1.4 and 1.5 are specially dealing with these two possibilities.

1.3 Equivalent circuit of induction machine using T-network

Now, it is possible to finally create equivalent circuit of induction machine using derived separation equations from previous chapter. All of the equivalent circuits have to meet following conditions:

1) they have to transfer equal power to recalculated load R'_L compared to original connection with original load R_L
2) both loaded circuits must have equal input impedance, which results directly from previous point
3) directly related to previous point, it is necessary for both loaded circuits to have equal time constants

This chapter is dealing with equivalent circuit using T-network. The same process of creating equivalent circuit will be followed in the next two chapters dealing with equivalent circuit using Γ-network or Ɪ-network, respectively. This procedure can be divided into three steps:

1) choosing the exact value of parameter σ
2) performing separation by substituting the chosen value of parameter σ into equations from (1.2-3) to (1.2-8)
3) recalculating rotor impedances $L_{\sigma 2}, R_2, R_L$ to the stator side as $L'_{\sigma 2}, R'_2, R'_L$ with square of transfer ratio (1.2-8) and substituting the chosen value of parameter σ

Following equations (1.3-1) – (1.3-3) serve to calculate values of recalculated parameters $L'_{\sigma 2}, R'_2, R'_L$ for any type of equivalent circuit (without choosing the value of parameter σ).

$$L'_{\sigma 2} = \frac{L_{\sigma 2}}{K^2_{h,V,21,0}} = L_1 \frac{1-k\sigma}{\sigma^2} \tag{1.3-1}$$

$$R'_2 = \frac{L_2}{K^2_{h,V,21,0}} = R_2 \frac{L_1}{\sigma^2 L_2} \tag{1.3-2}$$

$$R'_L = \frac{L_z}{K^2_{h,V,21,0}} = R_L \frac{L_1}{\sigma^2 L_2} \tag{1.3-3}$$

From *Pic. 1.3-1b* it is directly possible to define universal equation for calculation of voltage transfer at no-load state $K'_{V,21,0}$ of any type of equivalent circuit, as well.

$$K'_{U,21,0} = \frac{L_h}{L_h + L_{\sigma 1}} = \frac{k}{\sigma} \tag{1.3-4}$$

In this picture, there is illustrated a transition to equivalent circuit using T-network. Separated equivalent circuit of an induction machine can be found on the right side of the picture.

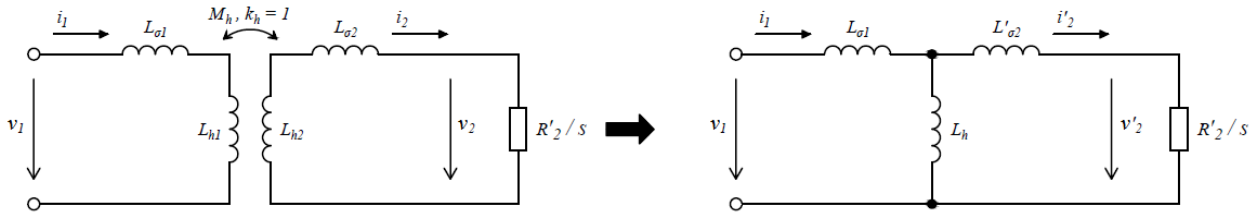

Pic. 1.3-1: T-separation (σ = 1); transition from separated connection to equivalent circuit.

It is necessary to choose the value of parameter $\sigma = 1$ in order to obtain classic induction machine equivalent circuit using T-network. By substituting this value into equations (1.2-3) – (1.2-8), a T-separation is obtained:

$$L_{\sigma 1} = L_1(1-k) \tag{1.3-s1}$$

$$L_{\sigma 2} = L_2(1-k) \tag{1.3-s2}$$

$$L_{h1} = kL_1 \tag{1.3-s3}$$

$$L_{h2} = kL_2 \tag{1.3-s4}$$

$$K_{h,V,21,0} = \sqrt{\frac{L_2}{L_1}} \tag{1.3-s5}$$

By further substitution of this value into equations (1.3-1) – (1.3-4), a symmetrical equivalent circuit of an induction machine using T-network is obtained, where $L_{\sigma 1} = L'_{\sigma 2}$:

$$L_{\sigma 1} = L_1(1-k) \tag{1.3-s6}$$

$$L'_{\sigma 2} = L_1(1-k) \tag{1.3-s7}$$

$$L_h = L_{h1} = kL_1 \tag{1.3-s8}$$

$$R'_L = R_L \frac{L_1}{L_2} \tag{1.3-s9}$$

$$K'_{V,21,0} = k \tag{1.3-s10}$$

From *Pic. 1.3*-1 it is obvious that after substitution for $L_{\sigma 1} = L'_{\sigma 2} = L_1(1-k)$ equivalent circuit is not analogous with stator of any model. Voltage transfer in no-load state of separated and original connection is different in coupling factor *k*.

Until now, we considered ideal induction machine without any parasitic elements, which means without losses. Now, it is possible to recalculate parasitic impedances from rotor side to

stator side by using square of known voltage transfer at no-load state $K_{h,V,21,0}$ (1.3-s5) and thus to create final equivalent circuit using T-network according to *Pic. 1.3-2*. By substituting value $\sigma = 1$ into equation (1.3-2), a value of resistance R'_2 recalculated to the stator side is obtained:

$$R'_2 = R_2 \frac{L_1}{L_2} \tag{1.3-s11}$$

In this moment, there are available values of all impedances (coming from equations (1.3-s6) – (1.3-s11)) creating equivalent circuit of an induction machine using T-network. The result is illustrated in *Pic. 1.3-2*.

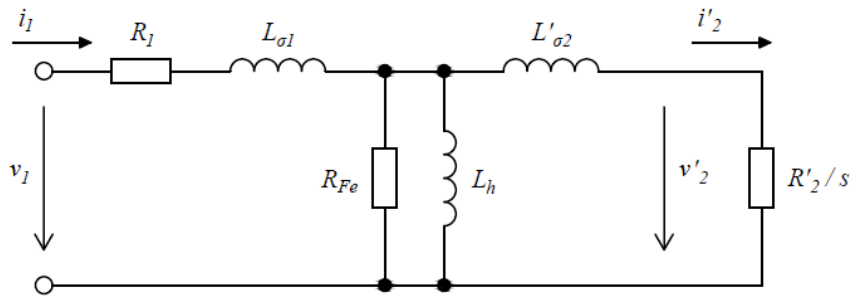

Pic. 1.3-2: Low-frequency equivalent circuit of an induction machine using T-network.

However, this type of equivalent circuit is in fact meaningless. It contains one more inductance compared to other connections (using Γ-network or Ί–network, respectively), thus it is unnecessarily complicated.

1.4 Equivalent circuit of induction machine using Γ-network

Equivalent circuit using Γ-network can be obtained by substituting first marginal value of inequality (1.2-10) as a value of parameter $\sigma = k$. Transition to equivalent circuit using Γ-network is illustrated in *Pic. 1.4-1*.

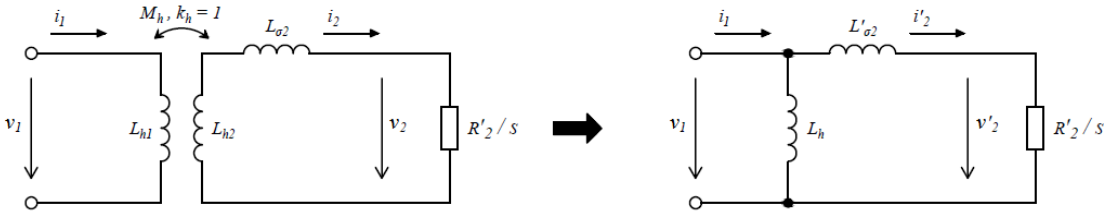

Pic. 1.4-1: Γ-separation (σ = k); transition from separated connection to equivalent circuit.

By substituting value of parameter $\sigma = k$ into equations (1.2-3) – (1.2-8), a Γ-separation is obtained:

$$L_{\sigma 1} = 0 \tag{1.4-s1}$$

$$L_{\sigma 2} = L_2(1 - k^2) \tag{1.4-s2}$$

$$L_{h1} = L_1 \tag{1.4-s3}$$

$$L_{h2} = k^2 L_2 \tag{1.4-s4}$$

$$K_{h,V,21,0} = k\sqrt{\frac{L_2}{L_1}} = K_{V,21,0} \tag{1.4-s5}$$

Similarly to previous subchapter, by further substitution of this value into equations (1.3-1) – (1.3-4), an equivalent circuit of an induction machine using Γ-network is obtained:

$$L_{\sigma 1} = 0 \tag{1.4-s6}$$

$$L'_{\sigma 2} = L_1 \frac{1-k^2}{k^2} \tag{1.4-s7}$$

$$L_h = L_{h1} = L_1 \tag{1.4-s8}$$

$$R'_L = R_L \frac{L_1}{k^2 L_2} \tag{1.4-s9}$$

$$K'_{V,21,0} = 1 \tag{1.4-s10}$$

A significant advantage of choosing a marginal value $\sigma = k$ of inequality (1.2-10) results directly from equation (1.4s6). In this case, inductance $L_{\sigma 1}$ equals zero and therefore the number of inductances in equivalent circuit is reduced to two.

Now, it is possible to recalculate parasitic impedances from rotor side to stator side by using square of known voltage transfer at no-load state $K_{h,V,21,0}$ (1.4-s5), and thus to create final equivalent circuit using Γ-network according to *Pic. 1.4-2*. By substituting value $\sigma = k$ into equation (1.3-2), a value of resistance R'_2 recalculated to the stator side, is obtained:

$$R'_2 = R_2 \frac{L_1}{k^2 L_2} \tag{1.4-s11}$$

In this moment, there are available values of all impedances (coming from equations (1.4-s6) – (1.4-s11)) creating equivalent circuit of an induction machine using Γ-network. The result is illustrated in *Pic. 1.4-2*.

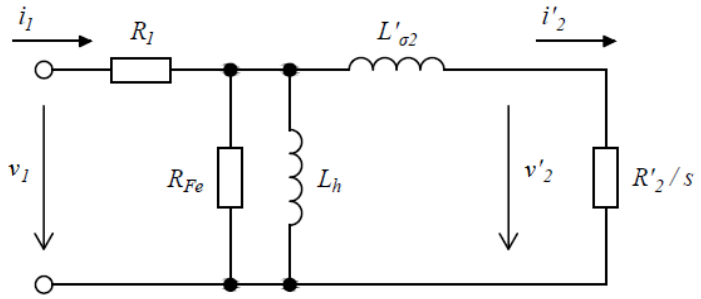

Pic. 1.4-2: Low-frequency equivalent circuit of an induction machine using Γ-network.

Use of this equivalent circuit is suitable in case when induction machine is powered from voltage source (for example vector control without current loops). As an example of use measuring of parameters can be presented – inductances and mutual inductances of squirrel-cage induction machines. In contradiction to induction machines with wound rotor, it is not possible to measure these parameters directly because no connection to the rotor circuits is possible. However, they can be obtained by measuring impedances of machine during no-load and short circuit test when the motor is powered just from voltage source. Measured parameters directly correspond to parameters of equivalent circuit of machine using Γ-network.

1.5 Equivalent circuit of induction machine using Ί-network

Equivalent circuit using Ί-network can be obtained by substituting second marginal value of inequality (1.2-10) as a value of parameter $\sigma = 1/k$. Transition to equivalent circuit using Ί-network is illustrated in *Pic. 1.5-1*.

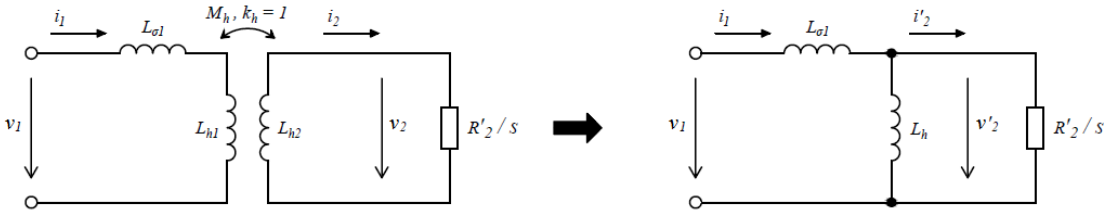

Pic. 1.5-1: Ί -separation ($\sigma = 1/k$); transition from separated connection to equivalent circuit.

By substituting value of parameter $\sigma = 1/k$ into equations (1.2-3) – (1.2-8), a Ί-separation is obtained:

$$L_{\sigma 1} = L_1(1 - k^2) \qquad (1.5\text{-s1})$$

$$L_{\sigma 2} = 0 \qquad (1.5\text{-s2})$$

$$L_{h1} = k^2 L_1 \qquad (1.5\text{-s3})$$

$$L_{h2} = L_2 \qquad (1.5\text{-s4})$$

$$K_{h,V,21,0} = \frac{1}{k}\sqrt{\frac{L_2}{L_1}} = \frac{1}{K_{I,21,K}} \qquad (1.5\text{-s5})$$

As in previous subchapters, by further substitution of value $\sigma = 1/k$ into equations (1.3-1) – (1.3-4), an equivalent circuit of an induction machine using Ί-network is obtained:

$$L_{\sigma 1} = L_1(1 - k^2) \tag{1.5-s6}$$

$$L'_{\sigma 2} = 0 \tag{1.5-s7}$$

$$L_h = L_{h1} = k^2 L_1 \tag{1.5-s8}$$

$$R'_L = R_L k^2 \frac{L_1}{L_2} \tag{1.5-s9}$$

$$K'_{V,21,0} = k^2 \tag{1.5-s10}$$

A significant advantage of choosing a marginal value $\sigma = 1/k$ of inequality (1.2-10) results directly from equation (1.5s7). In this case, inductance $L_{\sigma 2}$ (its recalculated value $L'_{\sigma 2}$, respectively) equals zero and so the number of inductances in equivalent circuit is reduced to two.

Now, it is possible to recalculate parasitic impedances from rotor side to stator side by using square of known voltage transfer at no-load state $K_{h,V,21,0}$ (1.5-s5), and thus to create final equivalent circuit using Ί-network according to *Pic. 1.5-2*. By substituting value $\sigma = 1/k$ into equation (1.3-2), value of resistance R'_2 recalculated to the stator side is obtained:

$$R'_2 = R_2 k^2 \frac{L_1}{L_2} \tag{1.5-s11}$$

In this moment, there are available values of all impedances (coming from equations (1.5-s6) – (1.5-s11)) creating equivalent circuit of an induction machine using Ί-network. The result is illustrated in *Pic. 1.5-2*.

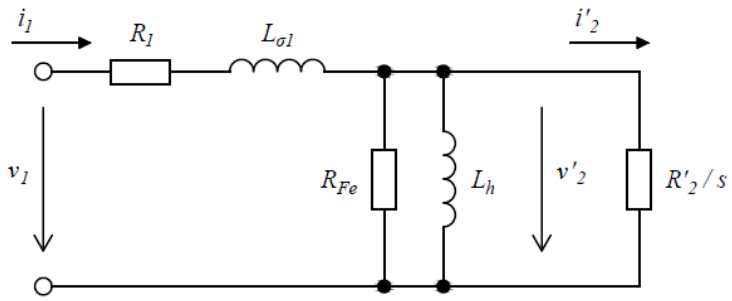

Pic. 1.5-2: Low-frequency equivalent circuit of an induction machine using Ί-network.

Use of this equivalent circuit is suitable in a case when induction machine is powered from current source (for example minor current loops in the structure of vector control).

2 THEORY OF VECTOR CONTROL

Vector control is a control method, originally developed mainly for applications, where following may be required: smooth machine operation over full speed range, generation of full torque at zero speed, or very fast acceleration/deceleration of machine. The principle of vector control of induction machines is to divide vector of stator current into two independent components with the help of suitable transformations and then control them independently. Moreover, one of these components is bound with creation of torque, whereas the second one is bound with creation of magnetic flux. Under any operational conditions, it is necessary to orientate the component of stator current bound with creation of magnetic flux to direction of vector motor magnetic flux. In the case when this component of stator current is oriented to:

a) *rotor magnetic flux*, then it is stated as rotor oriented vector control
b) *stator magnetic flux*, then it is stated as stator oriented vector control
c) *air-gap magnetic flux*, then it is stated as air-gap oriented vector control

The principle of rotor magnetic flux orientation is illustrated in *Pic. 2-1*, where the division of stator current vector can be seen. It is divided into two-phase stationary orthogonal reference frame $\alpha\beta$ bound with stator frequency of rotational magnetic field ω_1. This problem is to be discussed in next subchapter.

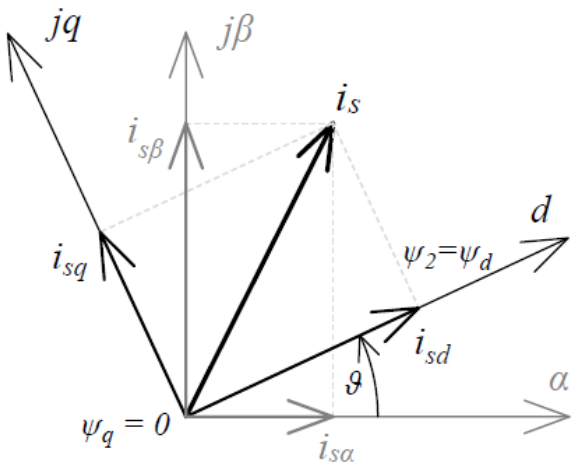

Pic. 1.5-1: Principle of rotor magnetic flux vector orientation.

All three methods of vector control have certain advantages under defined operational conditions. Therefore, all of them are been used.

It is possible to make a further division of vector control methods according to the process of acquiring information about magnitude and angle of magnetic flux. One type of control uses direct binding to the magnitude and angle of magnetic flux – this control type requires presence of magnetic flux sensor or estimator, respectively. Thus, we distinguish:

a) *direct vector control*, where either sensors of magnetic flux placed inside magnetic circuit of motor or estimator are used. From this estimator the information about magnitude and angle of magnetic flux are obtained, and transformation angle ϑ_k is acquired directly from these components.
b) *indirect vector control*, where calculation between both of the stator current components is used to obtain required slip frequency. Thereby, rotor magnetic flux vector orientation is achieved.

Rotor magnetic flux orientation is the most frequently used, no matter which type (direct or indirect) of control is preferred. The main reason is that this type of vector control is the only one where total detachment of both stator current components occurs. Due to problems with estimation of rotor magnetic flux in low speeds, there is often indirect vector control used instead. However, accuracy of this control type is dependent on changes of winding resistance with temperature. Therefore, in this case it is necessary to use estimator of resistance magnitude, as well.

2.1 Transformations of reference frames

To derive mathematical model of induction machine and design of regulation structure, it is necessary to define transformation relations. Block diagram in the *Pic. 2.1-1* (at the end of chapter) contains transformation blocks where input variables from the reference frame are transformed into variables defined in other reference frame. This reference frame is either two-phase system *αβ* bound with stator or two-phase system *dq* bound with stator frequency, respectively. Transformation equations from reference frame *abc* into reference frame *αβ* are known as Clarke's transformation. They are defined as follows:

$$i_\alpha = \frac{1}{3}(2i_a - i_b - i_c) = i_a \tag{2.1-1}$$

$$i_\beta = \frac{1}{\sqrt{3}}(i_c - i_b) \tag{2.1-2}$$

Inverse transformation from reference frame *αβ* into reference frame *abc*, commonly known as inverse Clarke's transformation, is proceeded using relations:

$$i_a = i_\alpha \tag{2.1-3}$$

$$i_a = -\frac{1}{2}i_\alpha - \frac{\sqrt{3}}{2}i_\beta \tag{2.1-4}$$

$$i_a = -\frac{1}{2}i_\alpha + \frac{\sqrt{3}}{2}i_\beta \tag{2.1-5}$$

Secondly used transformation in the block scheme of vector control is Park's transformation. It transforms variables from system *αβ* into sytem *dq* and it is defined as follows:

$$i_d = i_\alpha \cos\vartheta_k + i_\beta \sin\vartheta_k \tag{2.1-6}$$

$$i_q = -i_\alpha \sin\vartheta_k + i_\beta \cos\vartheta_k \tag{2.1-7}$$

Similarly to inverse Clarke's transformation, there also exists inverse Park's transformation. This transformation is used as reverse conversion of variables from system *dq* into system *αβ* and is defined by relations:

$$i_\alpha = i_d \cos\vartheta_k - i_q \sin\vartheta_k \tag{2.1-8}$$

$$i_\beta = i_d \sin\vartheta_k + i_q \cos\vartheta_k \tag{2.1-9}$$

A principle of these transformations is illustrated in *Pic. 2-1*. Detailed information involving this matter are to be found in literature [2].

2.2 Derivation of relations for mathematical model of induction machine; principle of rotor oriented vector control

Mathematical model of induction machine in this subchapter is derived using relations and conditions for rotor oriented vector control. The process comes from basic equations of generalized theory of electrical machine [3], while reference frame is bound with stator frequency:

$$\omega_k = \omega_1 \tag{2.2-1}$$

Voltage equations of general electrical machine in given reference frame are:

$$\bar{V}_1 = R_1\bar{\imath}_1 + \frac{d\bar{\psi}_1}{dt} + j\omega_1\bar{\psi}_1 \tag{2.2-2}$$

$$\bar{V}_2 = R_2\bar{\imath}_2 + \frac{d\bar{\psi}_2}{dt} + j(\omega_1 - p_p\omega)\bar{\psi}_2 = 0 \tag{2.2-3}$$

It is also necessary to state well-known motion equation for induction machine:

$$\frac{J}{p_p}\frac{d\omega}{dt} = \frac{3}{2}p_p \cdot Im\{\bar{\imath}_1\, x\, \bar{\psi}_1^*\} - m_z\ . \tag{2.2-4}$$

Last equations that we will come from are relations between magnetic fluxes and currents of stator and rotor. It is a couple of algebraic equations:

$$\bar{\psi}_1 = L_1\bar{\imath}_1 + L_h\bar{\imath}_2 \tag{2.2-5}$$

$$\bar{\psi}_2 = L_h\bar{\imath}_1 + L_2\bar{\imath}_2 \tag{2.2-6}$$

We will derive $\bar{\imath}_1, \bar{\psi}_2, \omega$ from known equation system with five variables where two couples are dependent on each other. By that, we eliminate remaining two variables $\bar{\imath}_2, \bar{\psi}_1$.

At first, we express $\bar{\imath}_2$ from equation (2.2-6) (relation (2.2-7)) and followingly substitute it into equation (2.2-5) (relation (2.2-8)) where we install first (so-called equivalent) parameter L_e (2.2-9):

$$\bar{\imath}_2 = \frac{1}{L_2}(\bar{\psi}_2 - L_h\bar{\imath}_1) = \frac{1}{L_2}\bar{\psi}_2 - \frac{L_h}{L_2}\bar{\imath}_1 \tag{2.2-7}$$

$$\bar{\psi}_1 = L_1\bar{\imath}_1 + \frac{L_h}{L_2}\bar{\psi}_2 - \frac{L_h^2}{L_2}\bar{\imath}_1 = \left(L_1 - \frac{L_h^2}{L_2}\right)\bar{\imath}_1 + \frac{L_h}{L_2}\bar{\psi}_2 \tag{2.2-8}$$

$$L_e = L_1 - \frac{L_h^2}{L_2} \tag{2.2-9}$$

These two expressed values $\bar{\imath}_2, \bar{\psi}_1$ will be further substituted into equations (2.2-2), (2.2-3) and (2.2-4) in order to eliminate dependent variables from these equations.

We substitute equation (2.2-8) into equation (2.2-2):

$$\bar{V}_1 = R_1\bar{\imath}_1 + \frac{d}{dt}\left(L_e\bar{\imath}_1 + \frac{L_h}{L_2}\bar{\psi}_2\right) + j\omega_1 L_e\bar{\imath}_1 + j\omega_1\frac{L_h}{L_2}\bar{\psi}_2 \tag{2.2-10}$$

Moreover, we substitute equation (2.2-7) into equation (2.2-3):

$$0 = \frac{R_2}{L_2}\bar{\psi}_2 - R_2\frac{L_h}{L_2}\bar{\imath}_1 + j(\omega_1 - p_p\omega)\bar{\psi}_2 + \frac{d\bar{\psi}_2}{dt} \tag{2.2-11}$$

where

$$\omega_2 = \omega_1 - p_p\omega \tag{2.2-12}$$

Similarly, we substitute equation (2.2-8) into equation (2.2-4):

$$\frac{J}{p_p}\frac{d\omega}{dt} = \frac{3}{2}p_p\,.\,Im\left\{\bar{\imath}_1\, x\, \left(L_e\bar{\imath}_1 + \frac{L_h}{L_2}\bar{\psi}_2\right)^*\right\} - T_L \tag{2.2-13}$$

In the next steps we will rearrange relations (2.2-10), (2.2-11) and (2.2-13).

It is possible to directly express time derivation of magnetic flux $\bar{\psi}_2$ from equation (2.2-11):

$$\frac{d\bar{\psi}_2}{dt} = -\frac{R_2}{L_2}\bar{\psi}_2 + R_2\frac{L_h}{L_2}\bar{\imath}_1 - j\omega_2\bar{\psi}_2 \tag{2.2-14}$$

We substitute equation (2.2-14) into equation (2.2-10) and after further rearrangement, we obtain:

$$\bar{V}_1 = \left[R_1 + R_2\left(\frac{L_h}{L_2}\right)^2\right]\bar{\imath}_1 - R_2\frac{L_h}{L_2^2}\bar{\psi}_2 + jp_p\omega\frac{L_h}{L_2}\bar{\psi}_2 + j\omega_1 L_e\bar{\imath}_1 + L_e\frac{d\bar{\imath}_1}{dt} \tag{2.2-15}$$

while we install second parameter – so-called equivalent resistance R_e (2.2-16). Although, this resistive parameter is also defined by inductances L_h, L_2, but at the first sight it is obvious that after their mutual quotient will dimensionless number remain. This number is used for recalculation of resistance R_2.

$$R_e = R_1 + R_2\left(\frac{L_h}{L_2}\right)^2 \tag{2.2-16}$$

From equation (2.2-15) we further express time derivation of current $\bar{\imath}_1$:

$$\frac{d\bar{\imath}_1}{dt} = \frac{1}{L_e}\left(-R_e\bar{\imath}_1 + \bar{V}_1 + R_2\frac{L_h}{L_2^2}\bar{\psi}_2 - jp_p\omega\frac{L_h}{L_2}\bar{\psi}_2\right) - j\omega_1\bar{\imath}_1 \tag{2.2-17}$$

We divide equation (2.2-13) into real and imaginary parts:

$$\frac{J}{p_p}\frac{d\omega}{dt} = \frac{3}{2}p_p\,.\,Im\left\{\left(i_{1d} + ji_{1q}\right)\, x\, \left[L_e i_{1d} + \frac{L_h}{L_2}\psi_{2d} - j\left(L_e i_{1q} + \frac{L_h}{L_2}\psi_{2q}\right)\right]\right\} - T_L \tag{2.2-18}$$

Imaginary component inside square brackets has negative sign because it is complex conjugate value. After rearrangement of this equation, we obtain following relation:

$$\frac{J}{p_p}\frac{d\omega}{dt} = \frac{3}{2}p_p\frac{L_h}{L_2}\left(\psi_{2d}i_{1q} - \psi_{2q}i_{1d}\right) - T_L \tag{2.2-19}$$

Final relations for mathematical model of induction machine in given reference frame are:

$$\frac{di_{1d}}{dt} = \frac{1}{L_e}\left(-R_e i_{1d} + V_{1d} + R_2 \frac{L_h}{L_2^2}\psi_{2d} + p_p \omega \frac{L_h}{L_2}\psi_{2q}\right) + \omega_1 i_{1q} \tag{2.2-20}$$

$$\frac{di_{1q}}{dt} = \frac{1}{L_e}\left(-R_e i_{1q} + V_{1q} + R_2 \frac{L_h}{L_2^2}\psi_{2q} - p_p \omega \frac{L_h}{L_2}\psi_{2d}\right) - \omega_1 i_{1d} \tag{2.2-21}$$

$$\frac{d\psi_{2d}}{dt} = R_2 \frac{L_h}{L_2} i_{1d} - \frac{R_2}{L_2}\psi_{2d} + \omega_2 \psi_{2q} \tag{2.2-22}$$

$$\frac{d\psi_{2q}}{dt} = R_2 \frac{L_h}{L_2} i_{1q} - \frac{R_2}{L_2}\psi_{2q} - \omega_2 \psi_{2d} \tag{2.2-23}$$

$$\frac{d\omega}{dt} = \frac{p_p}{J}\left[\frac{3}{2} p_p \frac{L_h}{L_2}\left(\psi_{2d} i_{1q} - \psi_{2q} i_{1d}\right) - T_L\right] \tag{2.2-24}$$

$$R_e = R_1 + R_2 \left(\frac{L_h}{L_2}\right)^2 \tag{2.2-25}$$

$$L_e = L_1 - \frac{L_h^2}{L_2} \tag{2.2-26}$$

$$\omega_2 = \omega_1 - p_p \omega \tag{2.2-27}$$

From equations (2.2-22) and (2.2-23), it is obvious that magnetic flux ψ_{2d} is excited by current i_{1d}. Similarly, flux ψ_{2q} is excited by current i_{1q}. This means that couples ψ_{2d}, i_{1d} and ψ_{2q}, i_{1q} have equal signs in every moment. By application of this information to equation (2.2-24) we discover that no matter what the conditions are, component $\psi_{2q} i_{1d}$ lowers final torque. Because of this we choose value of magnetic flux to be equal zero (ψ_{2q} = 0). Due to this fact, we can further assume that the time derivation of flux ψ_{2q} equals zero, as well. By substituting this condition into equations (2.2-20) - (2.2-24), the whole system will be significantly simplified together with reduction of their count:

$$\frac{di_{1d}}{dt} = \frac{1}{L_e}\left(-R_e i_{1d} + V_{1d} + R_2 \frac{L_h}{L_2^2}\psi_{2d}\right) + \omega_1 i_{1q} \tag{2.2-28}$$

$$\frac{di_{1q}}{dt} = \frac{1}{L_e}\left(-R_e i_{1q} + V_{1q} - p_p \omega \frac{L_h}{L_2}\psi_{2d}\right) - \omega_1 i_{1d} \tag{2.2-29}$$

$$\frac{d\psi_{2d}}{dt} = R_2 \frac{L_h}{L_2} i_{1d} - \frac{R_2}{L_2}\psi_{2d} \tag{2.2-30}$$

$$\frac{d\omega}{dt} = \frac{p_p}{J}\left(\frac{3}{2} p_p \frac{L_h}{L_2}\psi_{2d} i_{1q} - T_L\right) \tag{2.2-31}$$

Component of stator current i_{1q} is usually termed as torque-producing because it directly takes part in creation of torque of machine. It comes from equation (2.2-31). Component of stator current i_{1d} is similarly termed as flux-producing because it directly takes part in excitation of magnetic flux ψ_{2d}, what is obvious from equation (2.2-30). These facts are exactly analogous to DC machine with external excitation.

Thus, equation system (2.2-28) - (2.2-31) reminds relations of DC machine with external excitation. Parameters that make them to differ are exceeding cross-coupling bindings of current. From dynamic point of view, these bindings cause mutual influence of current values i_{1d}, i_{1q}.

In practice it means that by regulating one component of stator current, the other one is changed , as well. However, this effect has nearly no influence on the control of machine. It is because in both axes, the change is suppressed by current regulators.

However, there exists a possibility where this effect is totally eliminated by using so-called decoupling; specifically by adding compensating voltage V'_{1d} and V'_{1q} directly behind current regulators:

$$V'_{1d} = V_{1d} - L_e \omega_1 i_{1q} \tag{2.2-32}$$

$$V'_{1q} = V_{1q} + L_e \omega_1 i_{1d} \tag{2.2-33}$$

By backward use of these voltages, equations (2.2-28) and (2.2-29) will look as follows:

$$\frac{di_{1d}}{dt} = \frac{1}{L_e}\left(-R_e i_{1d} + V'_{1d} + R_2 \frac{L_h}{L_2^2}\psi_{2d}\right) \tag{2.2-34}$$

$$\frac{di_{1q}}{dt} = \frac{1}{L_e}\left(-R_e i_{1q} + V'_{1q} - p_p \omega \frac{L_h}{L_2}\psi_{2d}\right) \tag{2.2-35}$$

Zero value of magnetic flux ψ_{2q} = 0 is a condition for vector control. By application of this condition to equation (2.2-23) we obtain a relation that determines rotor angular velocity (2.2-36). After adding mechanical rotational speed of machine to this value, we obtain necessary stator frequency:

$$\omega_1 = \omega_2 + p_p \omega \tag{2.2-36}$$

$$\omega_2 = R_2 \frac{L_h}{L_2} \frac{i_{1q}}{\psi_{2d}} \tag{2.2-37}$$

In *Pic. 2.2-1*, there is illustrated block diagram of rotor magnetic flux oriented vector control of induction machine. Further, in chapter 4, a simulation model is created in MATLAB Simulink environment by using this specific diagram. This block diagram consists of induction machine, frequency inverter, four regulators (2 current, flux and speed), decoupling block, de-excitation.

Calculation block of presented control scheme is used for determining rotor magnetic flux ψ_{2d} (relation (2.2-30)) and for estimating stator frequency ω_1 (relations (2.2-36) and (2.2-37)). Transformation angle ϑ_k used for transformation of coordinate systems is defined as:

$$\vartheta_k = \frac{d\omega_1}{dt} \tag{2.2-38}$$

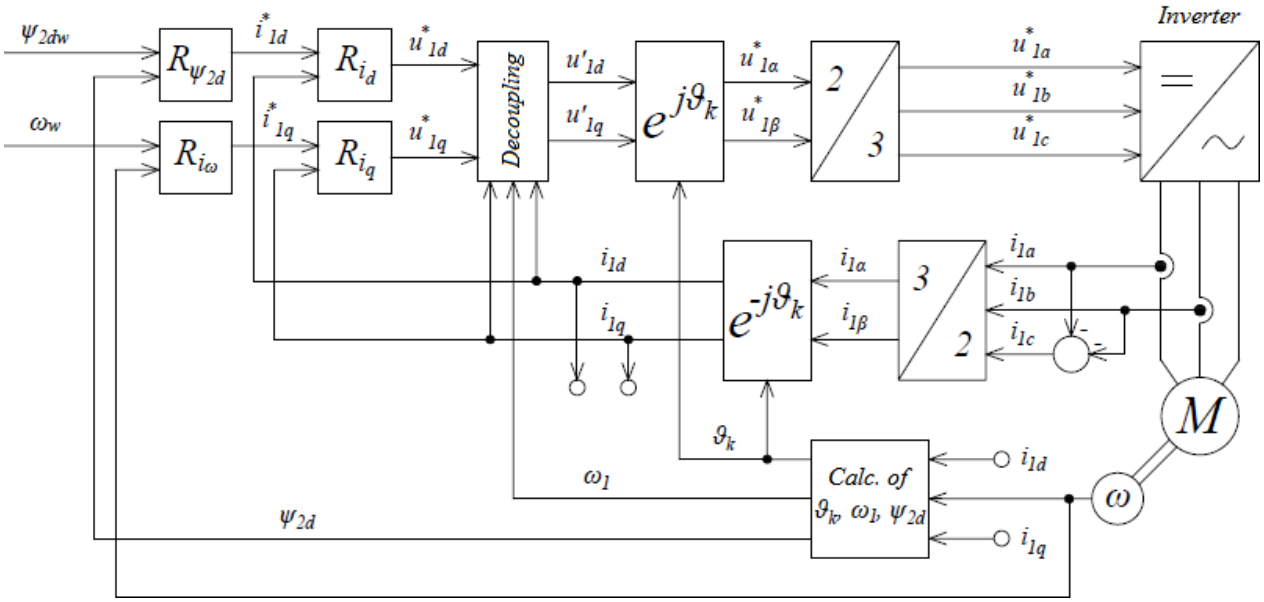

Pic. 2.2-1: Block diagram of rotor oriented vector control of induction machine.

At the first sight, this block diagram illustrated in picture above may seem to be rather complicated. However, it is quite simple in principle. The explanation will start at the bottom right part of the picture where the calculation block is placed. It covers feedback from induction machine to regulation structure by calculating transformation angle ϑ_k (used in transformation blocks), stator angular velocity ω_1 (used for decoupling) and estimated value of rotor magnetic flux ψ_{2d} (used as an input of magnetic flux regulator R_ψ). Stator current feedback structure can be found directly above calculation block. Measured currents are used as current regulators inputs, and in calculation and decoupling blocks. The last value used in feedback is mechanical angular velocity measured directly on the shaft of the machine.

These four feedback values used in regulators are controlled by comparison to required reference values. Reference values for first couple of regulators (flux and speed) are defined directly by user. Output values of these regulators represent reference values of stator current in both coordinate system axis *d* and *q* used as inputs of current regulators. Outputs of current regulators represent required voltage on stator terminals and are subsequently decoupled in decoupling block. Then, they are transformed into 3-dimensional reference frame *abc* and used in frequency inverter that supplies the controlled machine.

3 MODEL OF INDUCTION MACHINE, PWM MODULATOR AND INVERTER

This chapter is focused on step-by-step construction of control model basic elements – models of induction machine and PWM modulator with inverter. At the end of each subchapter, brief demonstrations of functionality of each created model will be presented.

3.1 Model of induction machine

The process of induction machine model creation comes from equations (2.2-25) - (2.2-31). Parameters used during the model assembly are listed in appendix at the end of this thesis. Resultant block model of induction motor created in Simulink environment is displayed in *Pic. 3.1-1*.

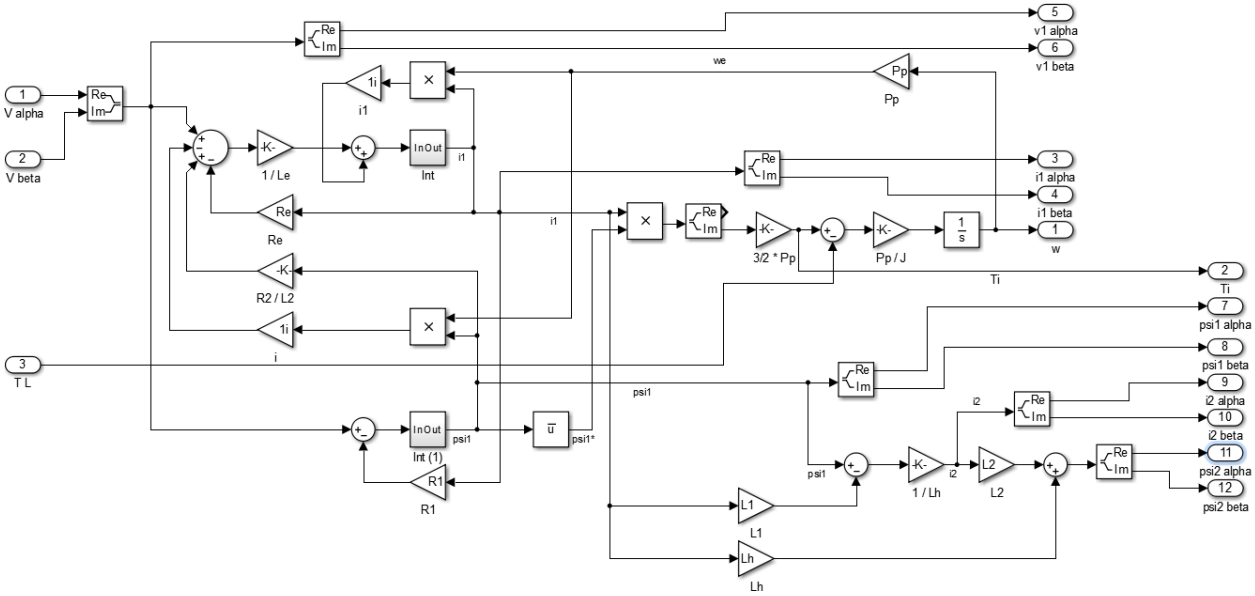

Pic. 3.1-1: Model of induction machine.

Nested blocks *Int* represent integration of two-dimensional input variable. Realization of this block can be seen in *Pic. 3.1-2* where each component of input signal is integrated separately and then the results are merged together into one signal.

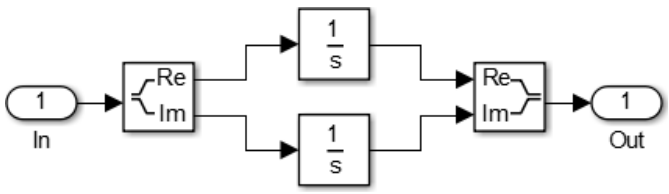

Pic. 3.1-2: Structure of nested block of integration Int.

This model of induction machine is slightly simplified compared to real one due to simplifying assumptions used during deriving of relations for this model. However, behavior of this model is sufficient for purposes of this thesis, so no further modifications are needed.

In *Pic. 3.1-3* it is possible to see time waveforms of angular velocity of motor and stator currents in reference frame $\alpha\beta$ after direct connection to the power utility system. Nominal load $T_L = 7\ Nm$ was connected at time $t = 0{,}3\ s$. It is possible to split the waveforms into four sections:

1) starting of non-loaded motor
2) steady state section
3) transient section after connecting nominal load
4) steady state section of loaded motor

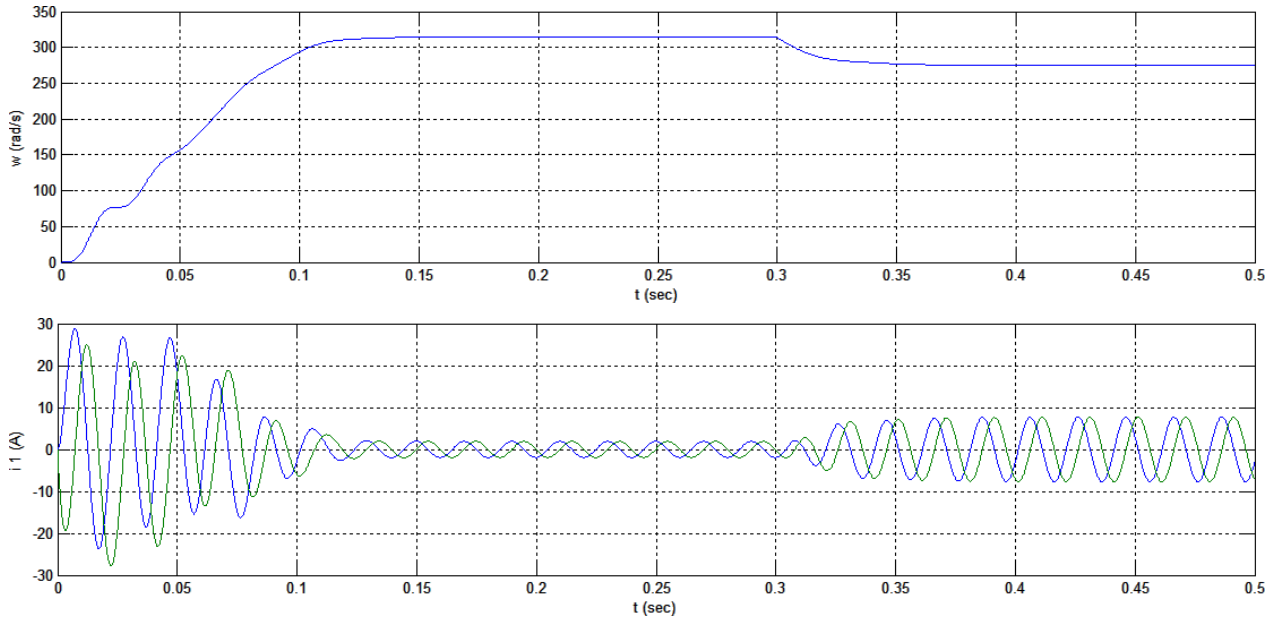

Pic. 3.1-3: Time waveforms of angular velocity and stator currents.

1) Angular velocity of non-loaded motor inside time interval $t \in < 0; 0{,}14 > s$ rises up to nominal value of 314 *rad/s* and the amplitude of stator current during starting lies slightly below 30 *A*. Non-fluent behavior of angular velocity during starting is caused by mechanical oscillations.
2) Amplitude of stator currents decreased to 2 *A* and angular velocity of motor remained still at nominal value.
3) Directly after connection of nominal load amplitude of stator currents started to increase to final value around 7,5 *A* and value of angular velocity slightly decreased to final 275 *rad/s*. This transient event lasted 0,06 *s*.

Model of induction machine is now complete and fully functional. The next step in creating model of any control type will be construction of model of PWM modulator with inverter.

3.2 PWM modulator and inverter

The most complicated part of control model created in this thesis is a model of PWM modulator with inverter. Realization of this model is projected in *Pic. 3.2-1*.

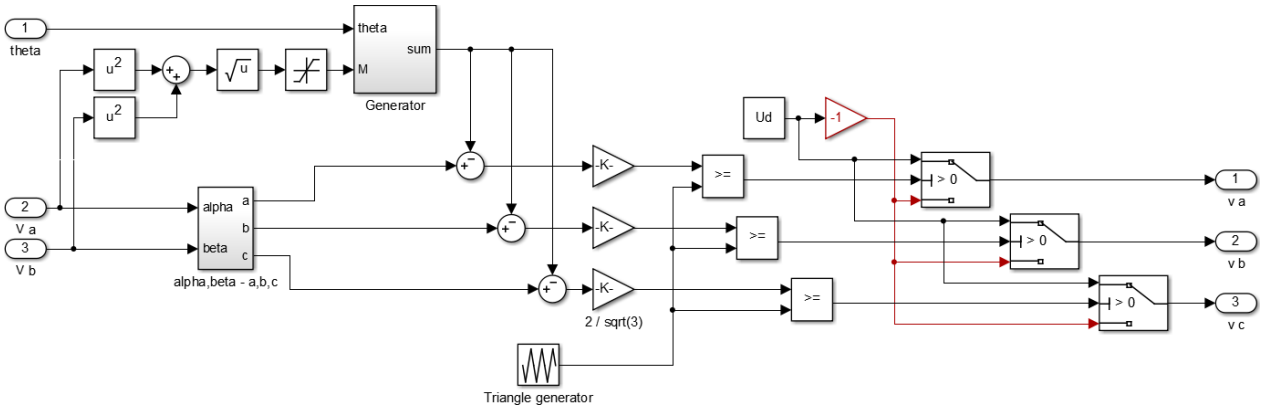

Pic. 3.2-1: Model of PWM modulator with inverter.

Explanation of operation principle is presented starting at the bottom left part of the picture (at the inputs 2 and 3). This way a signal enters from current regulators (slightly modified via decoupling block) in reference frame $\alpha\beta$ and is subsequently transformed to three-phase coordinate system *abc*. Function of following subtraction and multiplication blocks will be explained later. Three-phase signal is further compared to triangular high-frequency signal (usually 5-20 *kHz*). Outputs of these comparative blocks function as controlling pulses. These pulses control operation of following switches (in this model they are considered as ideal switches). Into the switches a half value of inverter DC bus voltage enters ($V_d/2$ = 270 *V*). Out of this value a negative value is produced, as well. The switches change the output value either to +270 *V* or to -270 *V* due to controlling signals of comparative blocks.

To achieve maximal possible value of first harmonic of output signal, it is necessary to add a signal to the original signal (for simple explanation, a sinusoidal waveform of original signal is considered). The added signal is created from 60-degree segments of original sinusoidal signal (segments from 60 to 120 degrees of a half-wave, specifically). Detailed analysis of this idea can be found in literature [4]. Principle of this idea is displayed in *Pic. 3.2-2*. However, it is necessary to emphasize that the added signal is definitely not a third harmonic of original signal, as it could seem at the first sight. The result of mutual summation of these two signals can be found in *Pic. 3.2-3*.

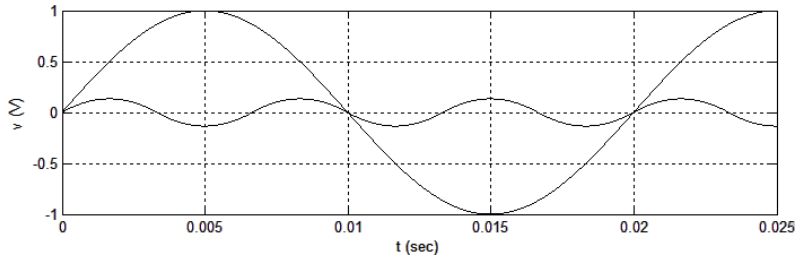

Pic. 3.2-2: Sinusoidal signal and signal created from 60-degree sinusoidal segments.

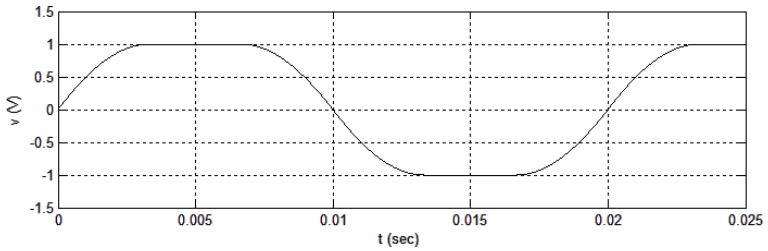

Pic. 3.2-3: Resultant signal after summation of signals in Pic. 3.2-2.

Creation of signal mentioned above consisting of 60-degree sinusoidal segments can be seen in the upper left corner in *Pic. 3.2-1*. This signal is created in block called *Generator* whose one of the inputs is a transformation angle ϑ. This angle is used for transforming signals from current regulators into reference frame $\alpha\beta$ and these signals subsequently enter into PWM modulator after decoupling (these are the input signals mentioned at the beginning of this subchapter – inputs 2 and 3). Structure inside the block *Generator* is operating with signals with amplitude equal 1, as we will see below. Therefore, it is necessary to modify amplitude of output signal to be corresponding with the original signal entering into PWM modulator. Second input of block *Generator* is according this explanation created by signal meaning amplitude of original input signal. This signal is obtained before second input of block *Generator* by a simple calculation using only two original input signals. Inner structure of block *Generator* is illustrated in *Pic. 3.2-4*.

Inside this block, three sinusoidal signals mutually shifted by 60 degrees are generated. It is essential for resultant output signal (60-degree segments) to move around zero. Therefore, constant $\sqrt{3}/2$ is subtracted/added to all of three generated sinusoidal signals. Resultant six signals are connected to six separate switches as one of the inputs. The second one is left unassigned (meaning this input value equals zero). These switches are used to "remove" (replace by zero value) everything from the signal but 60-degree required segments. The results from these switches are subsequently merged together and modified with amplitude mentioned above that enters into this block.

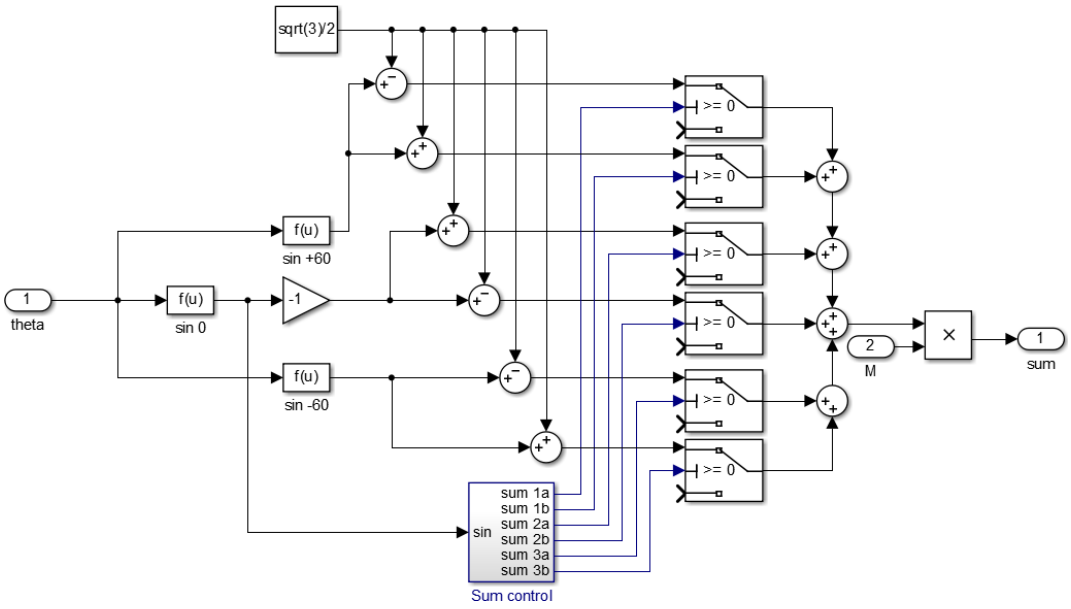

Pic. 3.2-4: Inner structure of block "Generator".

The six switches inside block Generator are controlled by block called *Sum control*. Structure of this block can be seen in *Pic. 3.2-5*. It is a logical block where:

- simple sinusoidal signal is compared to zero
- this identical signal is compared to value $\pm\sqrt{3}/2$
- monotony of this signal is observed (if it is increasing/decreasing)

These operations serve to define exact times for switching. An example of operation can be given using bottommost part of *Pic. 3.2-5*, where it is determined whether sinusoidal signal is:

- greater than zero
- smaller than $\sqrt{3}/2$
- decreasing

Considering these conditions, we see that they exactly define 60-degree segment (from 120 to 180 degrees) of original sinusoidal signal. Output signal is subsequently applied to switch sinusoidal signal shifted by -60 degrees. As a result, a 60-degree sinusoidal segment from negative half-wave is obtained.

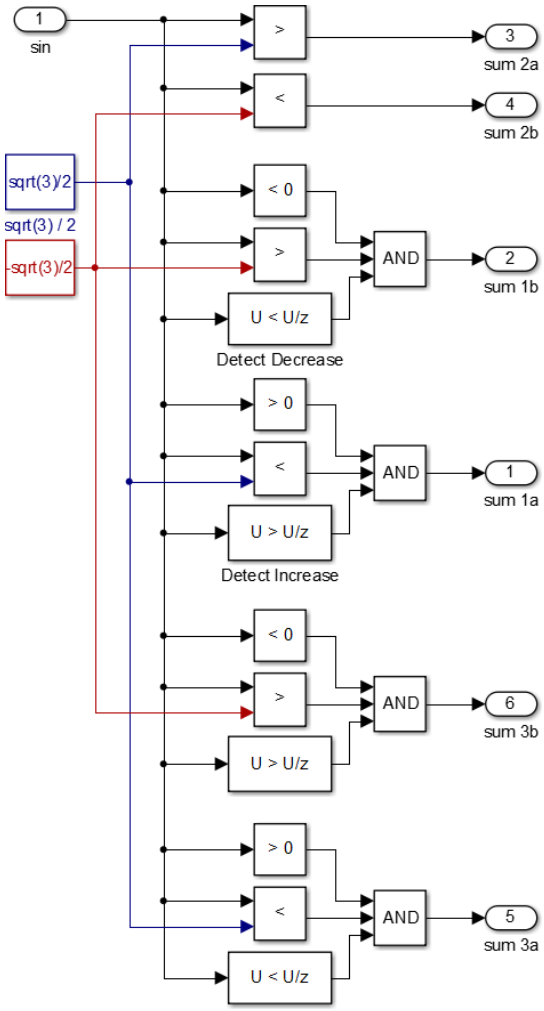

Pic. 3.2-5: Inner structure of nested controlling block "Sum control".

Now, if we look back at the *Pic. 5.3-1*, it is finally possible to explain those subtraction and multiplication blocks which were omitted during principle of operation explanation. Original signal is merged with generated one by subtraction blocks whereby original amplitude decreased $\sqrt{3}/2$ −times. Therefore, it is necessary to multiply the signal created by merging by value $2/\sqrt{3}$.

Examples of operation of constructed PWM modulator with inverter are to be found in *Pic. 3.2-6* and *Pic 3.2-7*. The first of mentioned pictures shows comparison for one phase - comparison of previously generated modulation signal (represented with blue color) with high-frequency triangular carrier signal (represented with green color) with frequency of 5 *kHz*. Resultant pulsating signal is represented with red color. Its three-phase time waveforms are displayed in *Pic. 3.2-7*.

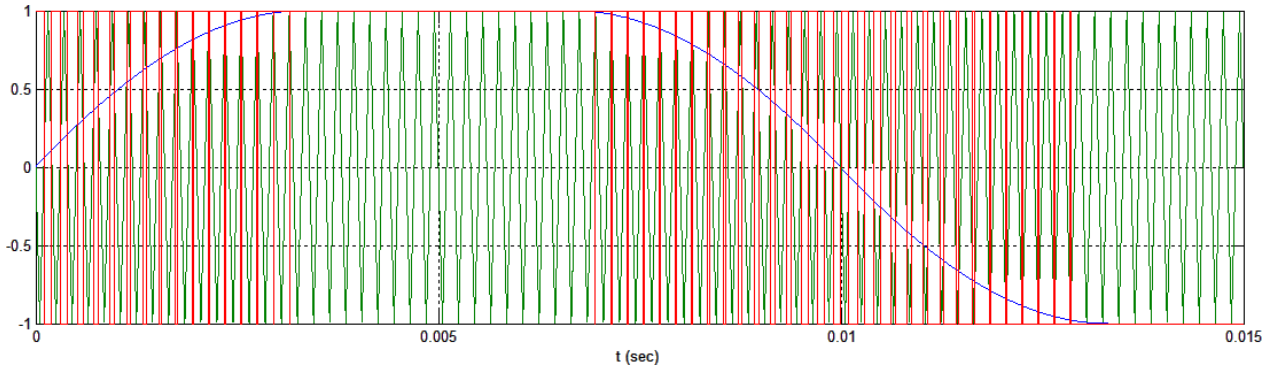

Pic. 3.2-6: Example of functionality of comparison inside PWM model.

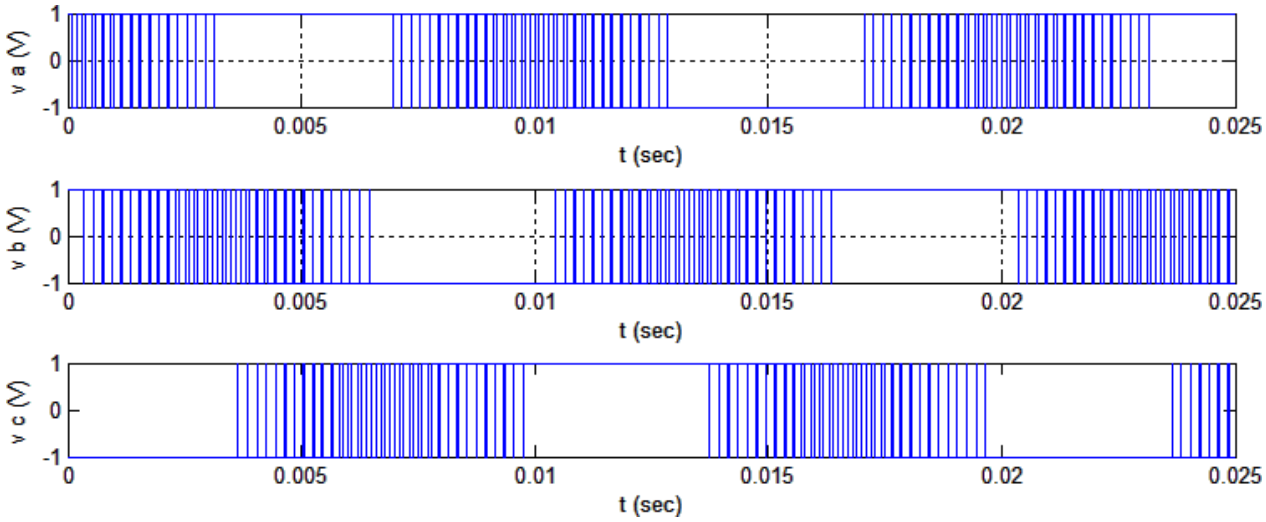

Pic. 3.2-7: Example of output signal coming from PWM modulator.

4 MODEL OF ROTOR ORIENTED VECTOR CONTROL

Complete model of induction machine rotor magnetic flux oriented vector control is illustrated in *Pic. 4-1*. At the first sight, it is evident that it is quite complicated system. Therefore, following subchapters will focus on more detailed description of individual blocks along with process of creation of this model. Blocks *IM* (model of induction machine) and *PWM* (model of PWM modulator with inverter) were already introduced in the previous chapter. Also, all four transformation blocks (*a,b,c-α,β; α,β-a,b,c; α,β-d,q; d,q-α,β*) were described earlier, as well. Remaining blocks that require detailed explanation are:

- 4 regulators (speed R_ω, magnetic flux R_ψ and 2 current R_i regulators)
- calculation block
- decoupling block
- de-excitation block

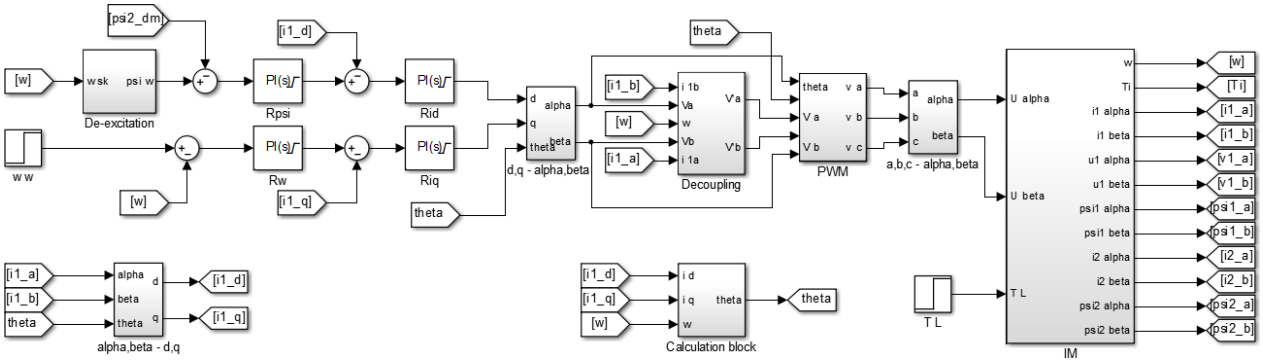

Pic. 3.2-1: Model of rotor oriented vector control created in Simulink environment.

4.1 Design of regulators

For proper functionality of control model of this type, it is necessary to accurately design all regulators. Therefore, this chapter is divided into other three following subchapters consecutively dealing with design of current, flux and speed regulators. During the process two basic design methods will be used - design method of optimal module or method of symmetrical optimum, eventually.

4.1.1 Design of current regulators

Design of current regulator R_i comes from equation (2.2-28). At first, we perform Laplace transform, whereby few elements in original equation were neglected. The result is expressed by relation (4.1.1-1).

$$L_e p I_{1d} = -R_e I_{1d} + V_{1d} \tag{4.1.1-1}$$

Relation (4.1.1-1) is further rearranged into form of transfer function:

$$F = \frac{I_{1d}}{V_{1d}} = \frac{1}{L_e p + R_e} = \frac{0{,}16}{3{,}03.10^{-3} p + 1} \tag{4.1.1-2}$$

In the next step, we will consider transfer of current sensor (4.1.1-3) and transfer of frequency inverter with gain $G = \frac{V_d}{2} = 270$ and time constant τ_{fi} = 50.10^{-6} what corresponds to switching frequency of inverter transistors at 20 *kHz*:

$$F_{si} = 1 \tag{4.1.1-3}$$

$$F_{fi} = \frac{270}{50.10^{-6}p + 1} \tag{4.1.1-4}$$

Transfer function F_S of whole system then equals:

$$F_S = F.F_{fi}.F_{si} = \frac{43{,}2}{(3{,}03.10^{-3}p + 1)(50.10^{-6}p + 1)} \tag{4.1.1-5}$$

Final value of current regulator R_i can be subsequently obtained by using design method of optimal module:

$$R_i = \frac{1}{2\tau_\sigma p\,(\tau_\sigma p + 1)} \cdot \frac{(3{,}03.10^{-3}p + 1)(50.10^{-6}p + 1)}{43{,}2} = \frac{3{,}03.10^{-3}p + 1}{4{,}32.10^{-3}p} \tag{4.1.1-6}$$

where time constant τ_{fi} was used as τ_σ.

It is possible to see that resultant regulator is PI-type. This regulator is used in the model in both axis (*d* and *q*, as well).

4.1.2 Design of magnetic flux regulator

At first, for a design of this regulator it is necessary to derive transfer function ψ_{2d}/i_{1d}. This process comes from equation (2.2-3), where a last element of this relation is neglected. Current $\overline{i_2}$ is expressed from equation (2.2-6) and subsequently substituted into already-mentioned simplified equation (2.2-3). Requested transfer function is then obtained:

$$\frac{d\psi_{2d}}{dt} = R_2 \frac{L_h}{L_2} i_{1d} - R_2 \frac{1}{L_2} \psi_{2d} \tag{4.1.2-1}$$

Moreover, Laplace transform is performed and after further rearrangement of created expression, we obtain desired form of transfer function:

$$F = \frac{\psi_{2d}}{i_{1d}} = \frac{L_h}{\frac{L_2}{R_2}p + 1} = \frac{0{,}3904}{0{,}11p + 1} \tag{4.1.2-2}$$

During calculation of transfer function F_S of whole system, the rest of the system will be for simplicity replaced by transfer function in form of first order system with time constant τ_{fi}:

$$F' = \frac{1}{2\tau_\sigma p + 1} = \frac{1}{2.50.10^{-6}p + 1} \tag{4.1.2-3}$$

Resultant transfer of whole system will then equal to:

$$F_S = F.F' = \frac{0{,}3904}{0{,}11p + 1} \cdot \frac{1}{10^{-4}p + 1} = \frac{0{,}3904}{(0{,}11p + 1)(10^{-4}p + 1)} \tag{4.1.2-4}$$

Design of magnetic flux regulator will be performed similarly to previous case by using design method of optimal module.

$$R_\psi = \frac{1}{2\tau_\sigma p\,(\tau_\sigma p + 1)} \cdot \frac{(0{,}11p + 1)(10^{-4}p + 1)}{0{,}3904} = \frac{0{,}11p + 1}{0{,}7808.10^{-4}p} \tag{4.1.2-5}$$

This resultant regulator is also PI-type likewise current regulator.

4.1.3 Design of speed regulator

The last designed regulator is a speed regulator R_ω. Process of this design comes from equation (2.2-31) where motor is considered non-loaded (that means load torque equals zero). Relation (4.1.3-1) is the result of Laplace transform:

$$p\omega = \frac{p_p^2}{J}\frac{3}{2}\frac{L_h}{L_2}\psi_{2d} i_{1q} \tag{4.1.3-1}$$

Moreover, simplifying assumption will be used in further steps – constant value of magnetic flux ψ_{2d} = 1 will be considered. From equation (4.1.3-1) is then simply expressed necessary transfer function ω/i_{1q}:

$$F = \frac{\omega}{i_{1q}} = \frac{1}{p}\frac{p_p^2}{J}\frac{3}{2}\frac{L_h}{L_2}\psi_{2d} = \frac{430{,}588}{p} \tag{4.1.3-2}$$

Transfer of the whole system is defined equally according to previous subchapter:

$$F_S = F.F' = \frac{430{,}588}{p}\cdot\frac{1}{10^{-4}p+1} = \frac{430{,}588}{p\,(10^{-4}p+1)} \tag{4.1.3-3}$$

In this case, design method of symmetrical optimum is more suitable in process of speed regulator design:

$$R_\omega = \frac{4\tau_\sigma p+1}{8\tau_\sigma^2 p^2\,(\tau_\sigma p+1)}\frac{p\,(10^{-4}p+1)}{430{,}588} = \frac{4.10^{-4}p+1}{34{,}447.10^{-6}p} \tag{4.1.3-4}$$

Equally to previous cases this resultant regulator is also PI-type.

4.2 Calculation block

Calculation block is very important part of the control model. It is used for feedback calculation of regulated value ψ_{2d}. Inner structure is very simple – it is created by relation (2.2-30) and equations (2.2-36) - (2.2-38). Final model created in Simulink environment is to be found in *Pic. 4.2-1*.

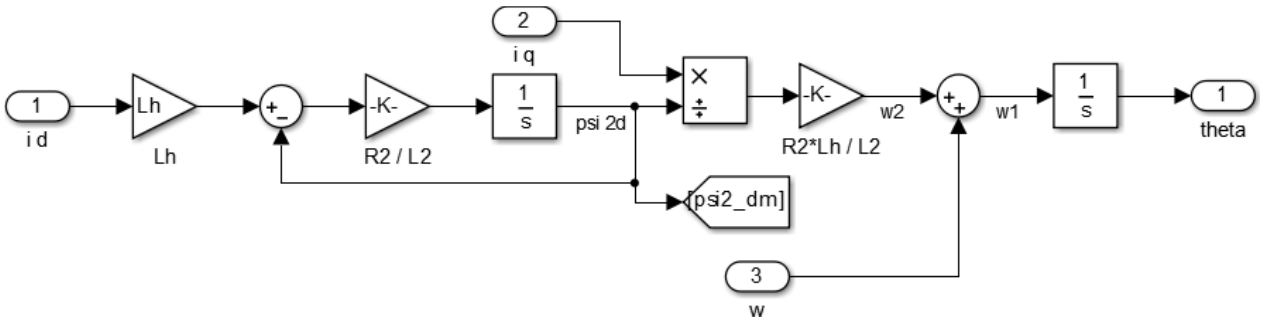

Pic. 4.2-1: Calculation block.

4.3 Decoupling block

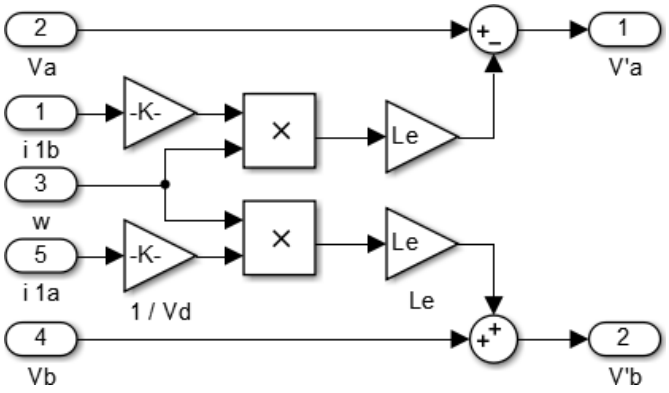

Pic. 4.3-1: Decoupling block.

Decoupling block is closely related to model of induction machine. Importance of this block was already discussed toward the end of second chapter. Inner structure of this block is created by equations (2.2-32) and (2.2-33) and is to be seen in *Pic. 4.3-1*. Its placement in control model can be found in *Pic. 4-1*, where it is possible to see that it is situated right before frequency inverter (block *PWM*).

4.4 De-excitation block

In this moment, the model of rotor oriented vector control is fully functional. However, one problem could occur in a case if required angular velocity is greater than nominal. Motor with value of nominal excitation given by constant (approximately equal 1) would not reach higher speed than nominal. Therefore, it is necessary to implement another block into model of control – so-called de-excitation block.

This block is monitoring actual mechanical angular velocity of motor and using this measured parameter to modify reference value of magnetic flux. When the motor with nominal excitation is approaching its nominal speed the de-excitation block is slowly decreasing reference value of magnetic flux ψ_{2d} (de-exciting) according to characteristics illustrated in *Pic. 4.4-2*. This characteristic was obtained using slightly modified indirect proportion $1/\omega$; in order to set the curve of characteristic and point where de-excitation starts to operate. Model of this block can be found in *Pic. 4.4-1*.

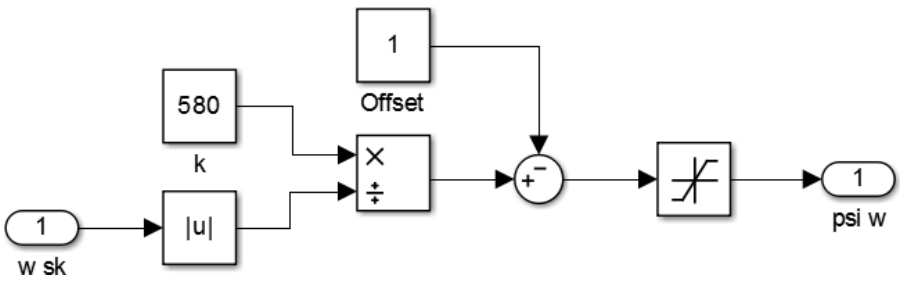

Pic. 4.4-1: De-excitation block.

Components called *Offset* and *k* are defining properties mentioned above of final characteristics. Moreover, block of absolute value ensures proper functionality of de-excitation even for opposite direction of mechanical revolutions. Last block used is a block of saturation that ensures two important values of characteristics:

- constant reference nominal value of magnetic flux for rotational speed lower than nominal (in this specific case starting point for de-excitation is placed a little bit lower at angular speed of 290 *rad/s*, specifically)
- lowest reference value of magnetic flux (at the highest impact of de-excitation)

These two values are during all simulations performed in this thesis set to $\psi_{2d\,h} = 1\ Wb$ and $\psi_{2d\,l} = 0{,}5\ Wb$.

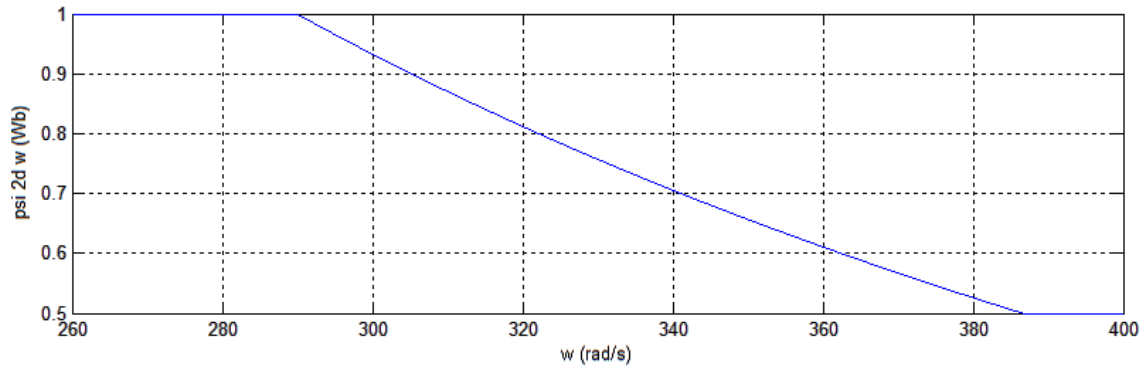

Pic. 4.4-2: Characteristics of de-excitation.

4.5 Results of simulation

Two simulations of rotor oriented vector control were performed – one without *PWM* block introduced above (this block was replaced with simple transfer function (4.1.1-4)), the second one along with this *PWM* block. At first, results of simplified simulation are presented.

Resultant time waveform of each parameter can be divided into 5 sections defined by given control conditions:

1) $t \in < 0; 0{,}05 >$: excitation of stationary motor – reference values: $\omega_w = 0\ rad/s$; $\psi_w = 1\ Wb$
2) $t \in < 0{,}05; 0{,}3 >$: starting of non-loaded fully excited motor – $\omega_w = 300\ rad/s$; $\psi_w = 1\ Wb$
3) $t \in < 0{,}3; 0{,}5 >$: connection of nominal load - $T_L = 7\ Nm$
4) $t \in < 0{,}5; 0{,}65 >$: unloading the motor - $T_L = 0\ Nm$
5) $t \in < 0{,}65; 0{,}8 >$: acceleration of motor to greater speed than nominal - $\omega_w = 400\ rad/s$

Time waveforms of mechanical angular velocity, voltage on stator terminals (in $\alpha\beta$ reference frame) and rotor magnetic flux (in *dq* reference frame) are to be found in *Pic. 4.5-1*. These waveforms were obtained during simulation without PWM modulator block constructed in previous chapter. Initial reference value of speed was set to zero in order to fully excite the motor before starting it up.

Reference value of angular speed was step changed to 300 *rad/s* at time 0,05 *s*. The motor is gradually accelerating until it reaches reference value. Magnetic flux slowly decreases (caused by de-excitation block), while the motor approaches reference value as it is defined by curve illustrated in *Pic. 4.4-2*.

Nominal value of load T_L = 7 *Nm* was further connected to the motor at time 0,3 *s*. It was subsequently disconnected at time 0,5 *s*. Just right after the connection there was a slight decrease in angular velocity for a short amount of time that was quickly regulated back to reference value. Both stator and rotor currents significantly increased after the load was connected. Voltage on stator terminals along with both magnetic fluxes (stator and rotor) slightly increased, as well. This event can be observed in *Pic 4.5-1* and *Pic. 4.5-3*. Component of rotor magnetic flux in axis *q* (green curve) is constantly preserved at zero value what we can see in the bottommost waveform illustrated in *Pic. 4.5-1*. This proves the correctness of control operation of the model.

All waveforms returned to the non-loaded state after disconnection of load (their characteristics are completely identical to those in second section).

Rotational speed of motor subsequently increases after the reference value of angular speed rose to 400 *rad/s* at time 0,65 *s*. During this process, it is obvious that the motor is gradually de-excited. Significant influence of regulators during transient events can be clearly seen in resultant waveforms, as well. They can be easily recognized by short oscillations in voltage or current waveforms.

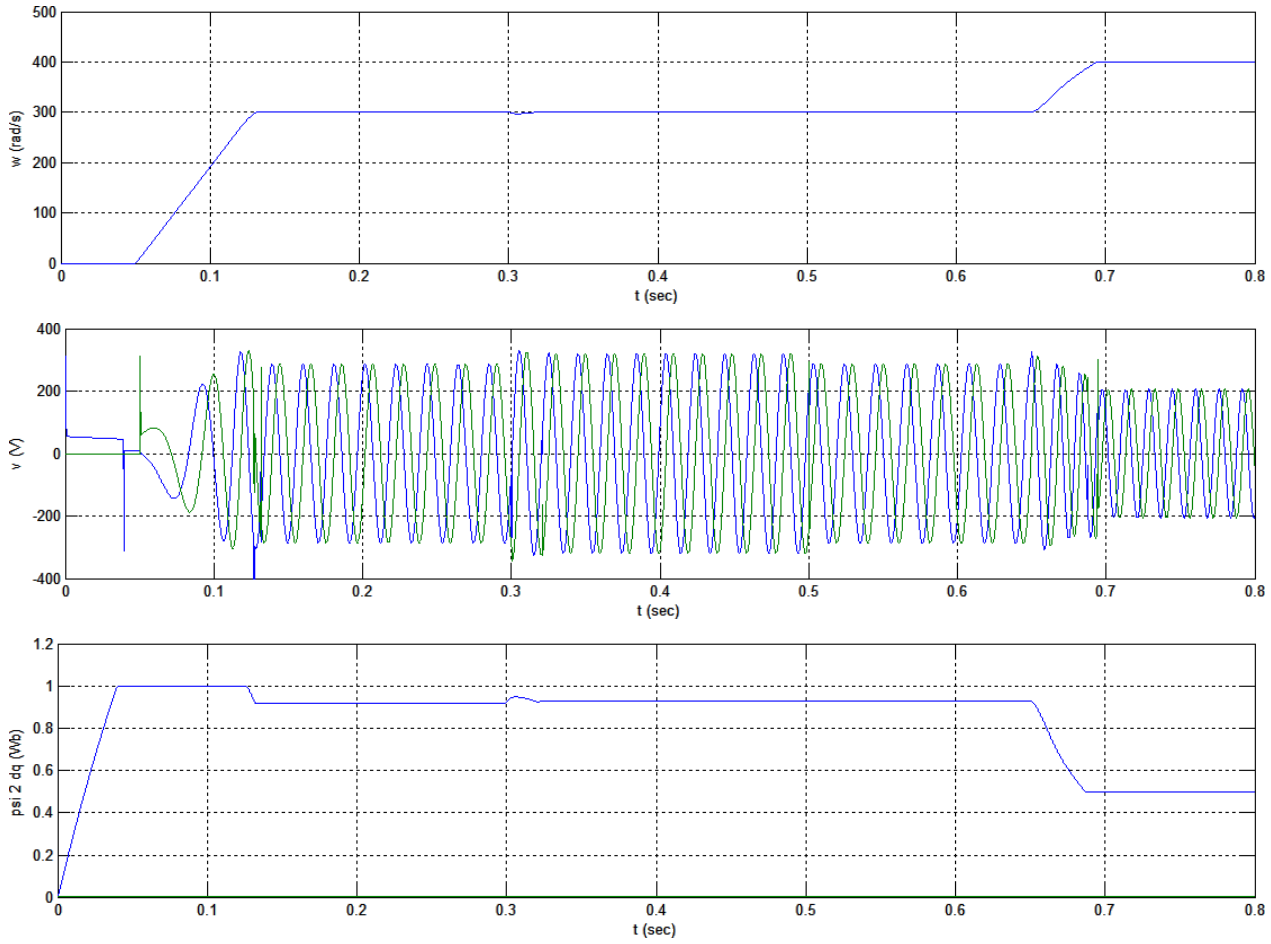

Pic. 4.5-1: Time waveforms of ω, v_1 in system αβ and ψ_2 in system dq without PWM modulation.

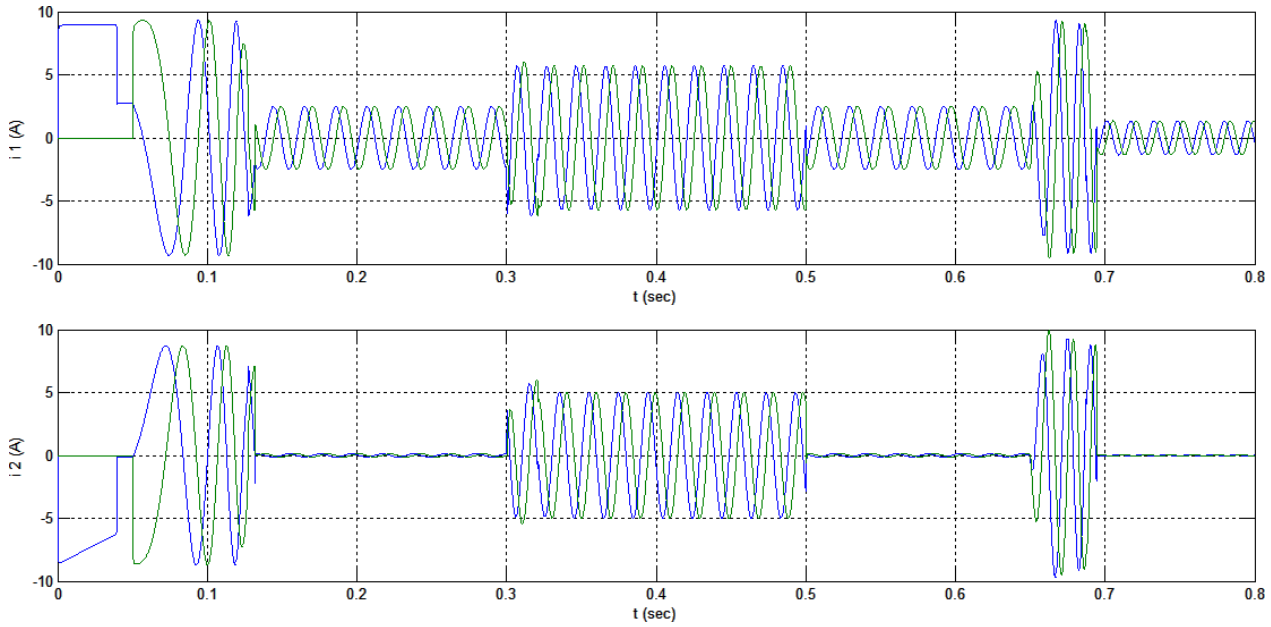

Pic. 4.5-2: Time waveforms of currents i_1 and i_2 in system αβ without PWM modulation.

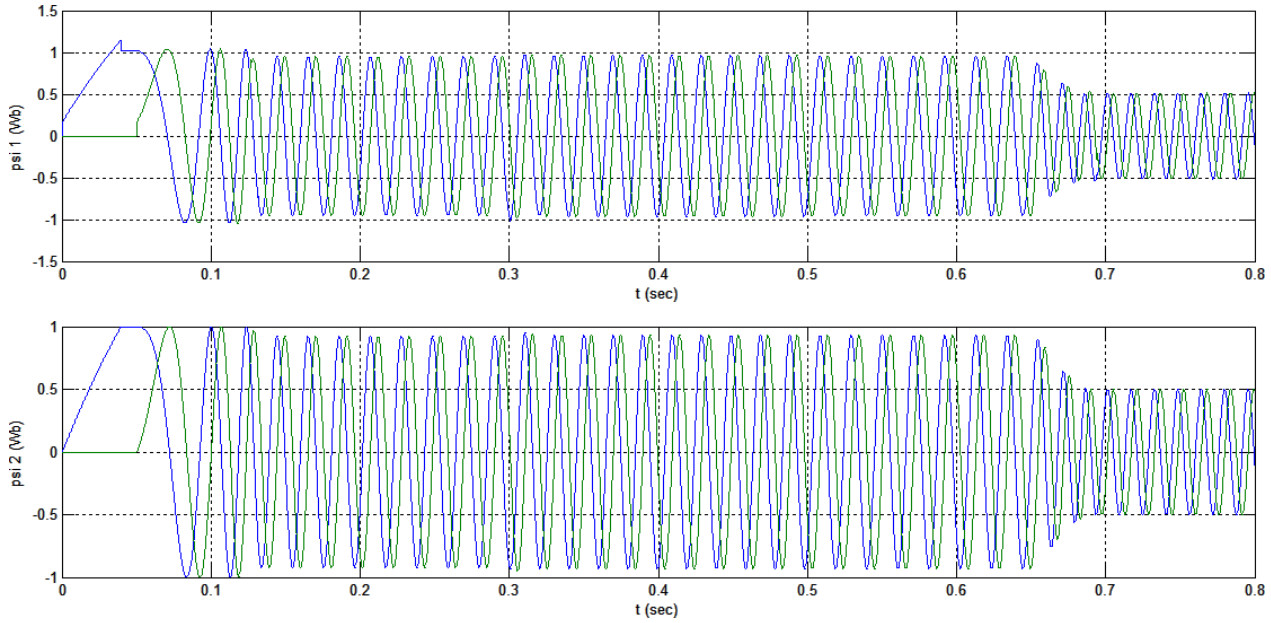

Pic. 4.5-3: Time waveforms of magnetic fluxes ψ_1 and ψ_2 in system αβ without PWM modulation.

Resultant waveforms of nearly all parameters created during simulation with PWM modulator with inverter attached to the control model were almost identical to those without PWM modulator. This was caused due to inductances that suppressed the influence of current ripple and made those waveforms smoother. The only exceptions were waveforms of both currents (stator and rotor) illustrated in *Pic. 4.5-4* and voltage at stator terminals, of course. However, this voltage is not presented because it is not possible to evaluate its waveform without sufficient zooming in. It is caused because it just consists of pulses performed at high frequency.

Waveforms of both currents i_1 and i_2 are nearly identical to those without PWM modulation, as well. The only difference is caused by triangular ripple of these waveforms. Detail of saw-tooth ripple of current i_1 is illustrated in *Pic. 4.5-5*. It was already mentioned that this ripple is suppressed by motor inductances and the result is smooth waveforms of mechanical rotations and all other parameters illustrated above.

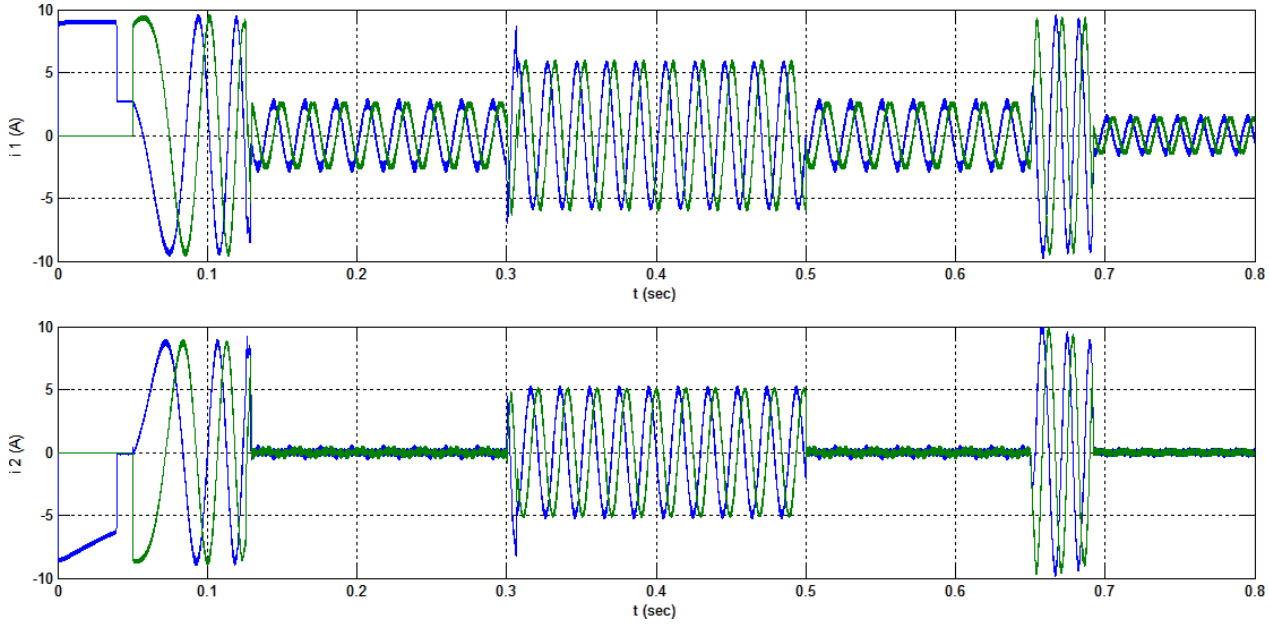

Pic. 4.5-4: Time waveforms of saw-tooth rippled currents i_1 and i_2 in system αβ.

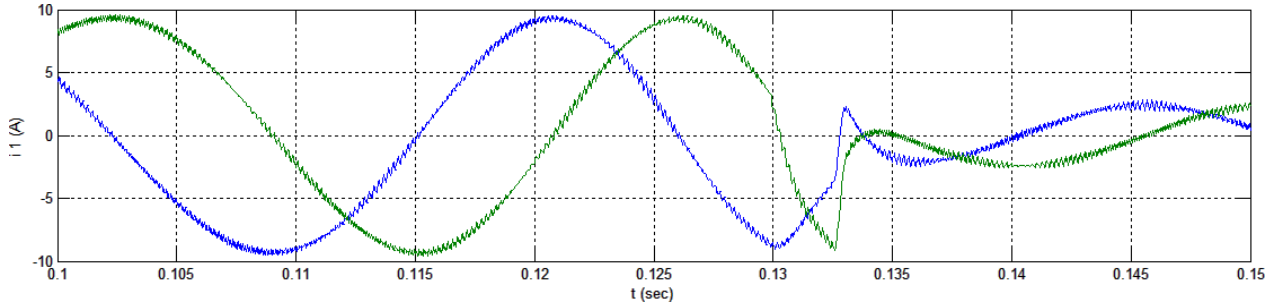

Pic. 4.5-5: Detail of current i_1 waveform.

5 MODEL OF STATOR ORIENTED VECTOR CONTROL

The only difference between stator and rotor oriented vector control is a magnetic flux of which part of induction machine is controlled. It is quite complicated to derive needed equations for rotor-oriented control mentioned above. However, stator magnetic field can be altered directly by voltage on terminals and stator current.

It is possible to create model of stator oriented vector control of induction machine just with slight modifications of rotor oriented vector control model created in previous chapter. Majority of blocks in Simulink environment will remain untouched. Model of this type of control is essentially identical to model illustrated in *Pic. 4-1*. The only change will be the calculation block where it is necessary to estimate value of stator magnetic flux ψ_{1d} (not ψ_{2d} as in that mentioned model) along with angular velocity ω_1 and transformation angle ϑ. The calculated stator magnetic flux ψ_{1d} is used in feedback structure as input of flux regulator R_ψ instead of rotor magnetic flux ψ_{2d} used in the control model described before.

5.1 Derivation of stator oriented vector control relations.

Derivation of equations for stator oriented vector control comes from relation (2.2-4). It is possible to easily express instant value of produced torque of induction machine directly from this equation:

$$T_i = \frac{3}{2} \cdot Im\{\bar{\imath}_1 \; x \; \bar{\psi}_1^*\} \tag{5.1-1}$$

Moreover, we will divide relation (5.1-1) into real and imaginary parts:

$$T_i = \frac{3}{2} \cdot Im\{(i_{1d} + j i_{1q}) \; x \; (\psi_{1d} - j\psi_{1d})\} \tag{5.1-2}$$

Imaginary component inside square brackets has negative sign because it is complex conjugate value. After rearrangement of relation (5.1-2) we obtain:

$$T_i = \frac{3}{2}(\psi_{1d} i_{1q} - \psi_{1q} i_{1d}) \tag{5.1-3}$$

Using exactly the same procedure as in chapter 2.2, it is possible to determine that couples ψ_{1d}, i_{1d} and ψ_{1q}, i_{1q} have equal signs in every moment. Similarly to rotor oriented control, the result of this information is that component $\psi_{1q} i_{1d}$ lowers final torque produced by motor under any operational conditions. Due to this fact, it is necessary to constantly preserve the value of stator magnetic flux ψ_{1q} in q axis at zero. Consequence of this fact is that time derivation of this magnetic flux will be equal zero, as well. This information is used during further derivation of equations.

Component of stator voltage v_1 in axis q is acquired by expressing it from equation (2.2-2):

$$V_{1q} = \frac{d\psi_{1q}}{dt} + R_1 i_{1q} + \omega_1 \psi_{1d} \tag{5.1-4}$$

Magnetic flux ψ_{1q} and its time derivation equal zero according to the explanation above. The relation (5.1-4) is then simplified into form:

$$V_{1q} = R_1 i_{1q} + \omega_1 \psi_{1d} \tag{5.1-5}$$

Important relation for calculation of angular velocity ω_1 is obtained by simple rearrangement of this equation:

$$\omega_1 = \frac{u_{1q} - R_1 i_{1q}}{\psi_{1d}} \tag{5.1-6}$$

Now, it is finally possible to start the creation of block model in Simulink environment.

5.2 Calculation block

This block is the only different block that is used in model of stator oriented vector control compared to rotor oriented vector control. Its creation comes from equation (5.1-6). However, calculation of magnetic flux ψ_{1d} is needed for its complete realization. It is easily acquired after decomposition of equation (2.2-5) into components:

$$\psi_{1d} = L_1 i_{1d} + L_h i_{2d} \tag{5.2-1}$$

Now, it is not a problem to construct calculation block. Its inner structure is illustrated in *Pic. 5.2-1*.

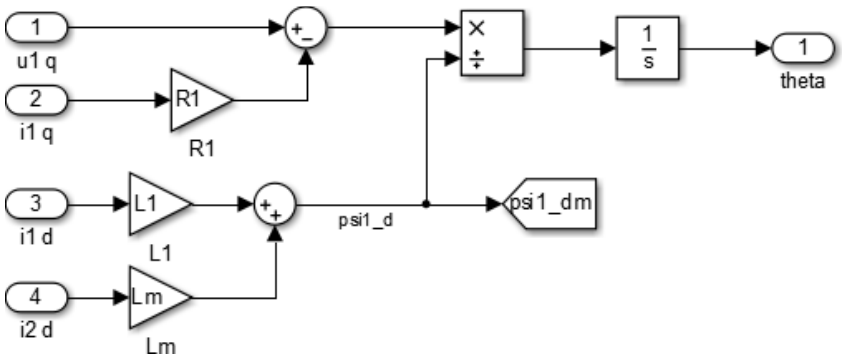

Pic. 5.2-1: Calculation block.

5.3 Results of simulation

By comparing simulation results of rotor oriented vector control with and without PWM modulator (chapter 4.5), it was possible to see that most of the final waveforms were not influenced by this modulator when used. The only difference between those two simulations is that waveforms of currents i_1 and i_2 were slightly saw-tooth rippled. Therefore, due to high requirements on hardware resources and very long calculation time of the simulation, use of PWM modulator will be omitted in further simulations.

Simulation of stator oriented vector control was performed using the exactly same control conditions as in previous chapter. All of the resultant waveforms are quite similar to those obtained during simulation of rotor oriented vector control. Due to this fact, only brief description is given (detailed description can be found in previous chapter). Mutual comparison of resultant waveforms obtained during rotor and stator oriented vector control is presented just right after demonstration of following results.

Due to same control conditions, it is also possible to divide resultant time waveforms of each parameter into the same 5 sections:

1) $t \in < 0; 0{,}05 >$: excitation of stationary motor – reference values: $\omega_w = 0$ *rad/s*; $\psi_w = 1$ *Wb*
2) $t \in < 0{,}05; 0{,}3 >$: starting of non-loaded fully excited motor – $\omega_w = 300$ *rad/s*; $\psi_w = 1$ *Wb*
3) $t \in < 0{,}3; 0{,}5 >$: connection of nominal load - $T_L = 7$ *Nm*
4) $t \in < 0{,}5; 0{,}65 >$: unloading the motor - $T_L = 0$ *Nm*
5) $t \in < 0{,}65; 0{,}8 >$: acceleration of motor to greater speed than nominal - $\omega_w = 400$ *rad/s*

Time waveforms of mechanical angular velocity, voltage on stator terminals (in *αβ* reference frame) and stator magnetic flux (in *dq* reference frame) are to be found in *Pic. 5.3-2*. As stated above, these waveforms are quite similar to those for rotor oriented control illustrated in *Pic. 4.5-1*. The motor was gradually accelerating to reference value 300 *rad/s*. In addition, a magnetic flux slowly decreased to the end of starting up (according to curve illustrated in *Pic. 4.4-2*).
Equally to simulation in chapter four, there was connected nominal value of load $T_L = 7$ *Nm* to the motor at time 0,3 *s* and subsequently disconnected at time 0,5 *s*. After the connection, a slight decrease in angular velocity for a short amount of time is present, as well. Voltage on stator terminals, both magnetic fluxes and both currents also increased after the load was connected. In the last graph in *Pic. 5.3-2*, there can be seen that component of stator magnetic flux in axis *q* (green curve) is similarly to previous vector control simulation constantly preserved at zero value what proves again the correctness of control operation of the model.
In the last section, where reference value of speed raised to 400 *rad/s*, rotational speed of motor subsequently increased. There can be also seen influence of de-excitation during this process.

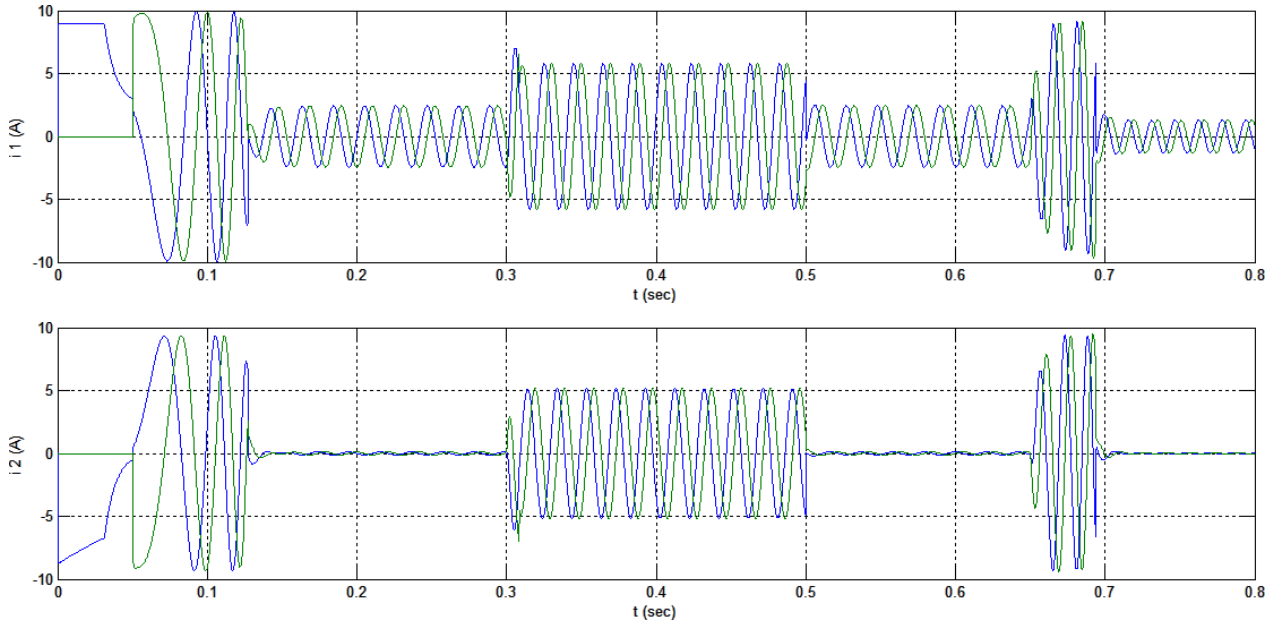

Pic. 5.3-1: Time waveforms of currents i_1 and i_2 in system αβ.

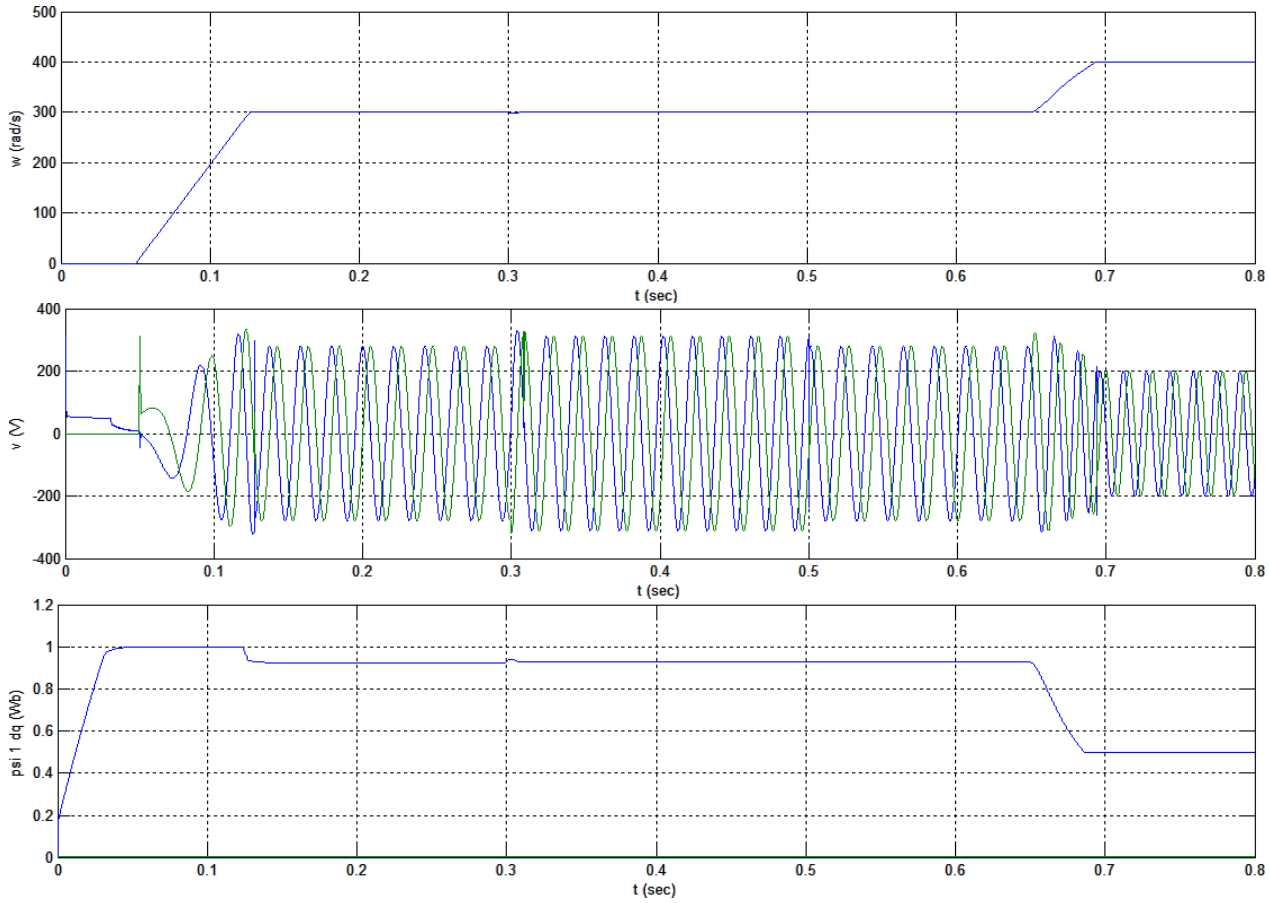

Pic. 5.3-2: Time waveforms of ω, v_1 in system αβ and ψ_1 in system dq.

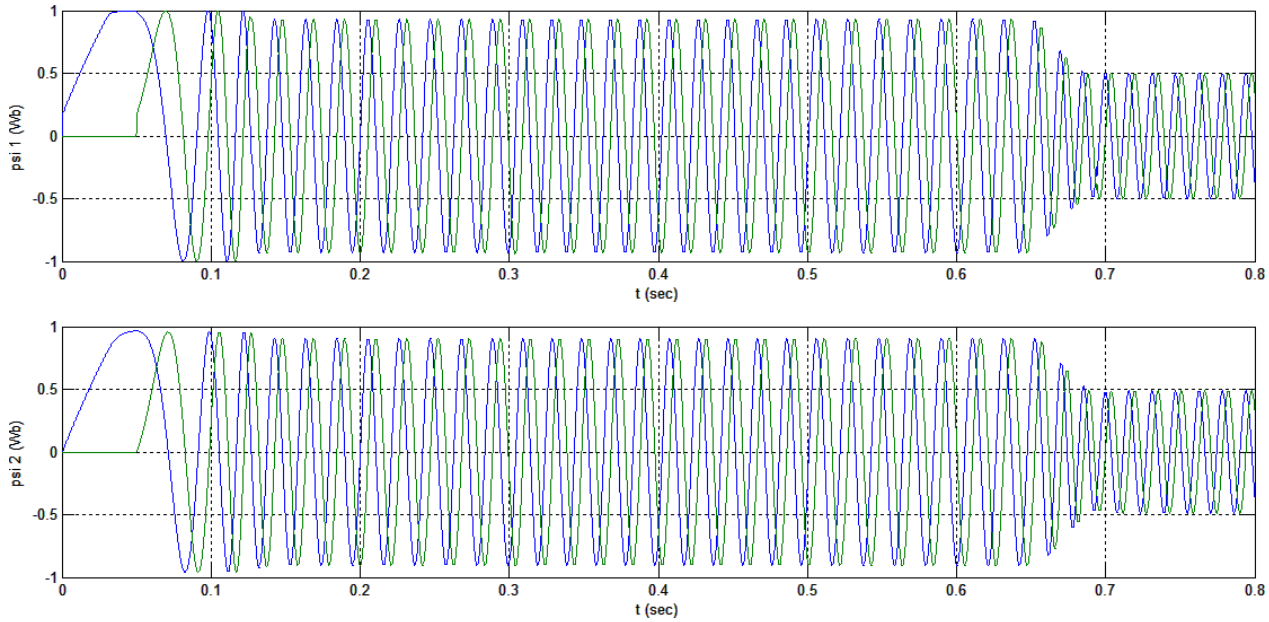

Pic. 5.3-3: Time waveforms of magnetic fluxes ψ_1 and ψ_2 in system αβ.

5.4 Comparison of results

This brief subchapter is focused on comparing the results of rotor and stator oriented vector control. Couples of waveforms of individual parameters will be consecutively introduced and differences between their properties discussed. The upper waveform will always belong to rotor-oriented control and the second one to stator-oriented control.

5.4.1 Comparison of mechanical angular velocity

In *Pic. 5.4-1*, illustrated below, waveforms of angular velocity obtained from simulations of rotor and stator oriented vector control can be seen . The results might seem to be identical at the first sight. However, stator oriented control provided faster start of the motor and its increase of speed to 400 *rad/s*, as well:

- angular velocity from 0 to 300 *rad/s* was reached 3 *ms* earlier
- increase in speed to value 400 *rad/s* was performed 2 *ms* earlier

These differences are not very noticeable but they would be more significant for bigger machines.

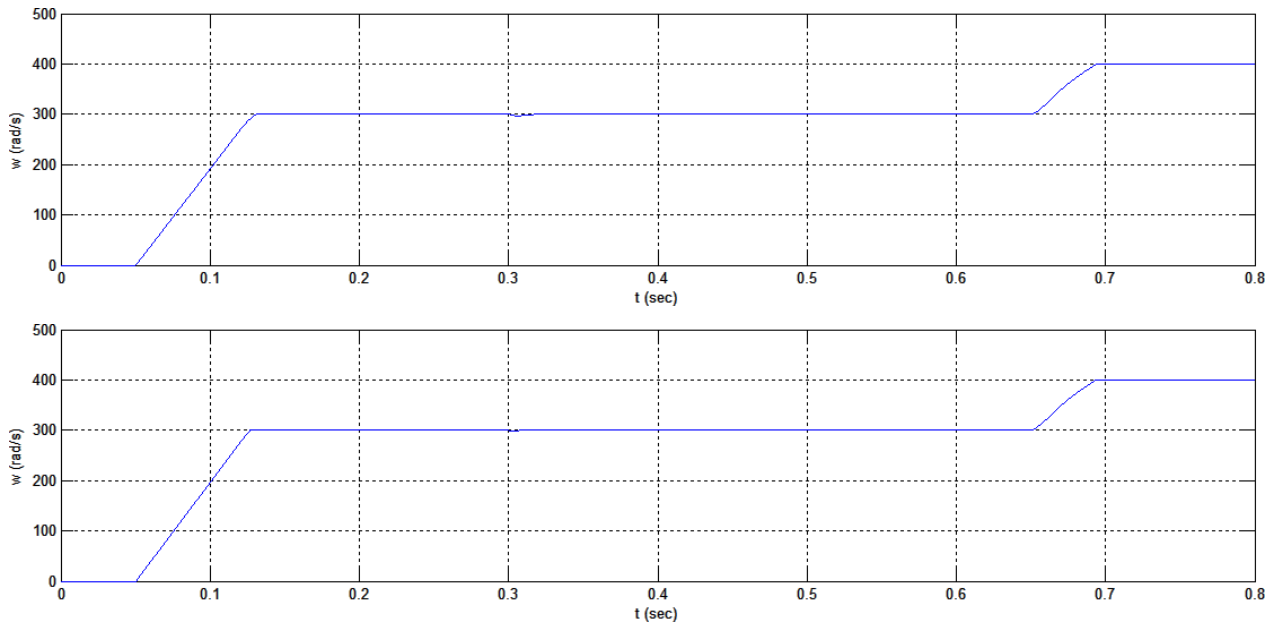

Pic. 5.4-1: Comparison of mechanical angular velocity.

5.4.2 Comparison of voltage on stator terminals

Waveforms of voltages on stator terminals in *Pic. 5.4-2* are also very similar. In this case, stator oriented vector control achieves lower values of input voltage, again. Voltage differences are:

- 7 *V* at no-load state
- 8 *V* with nominal load

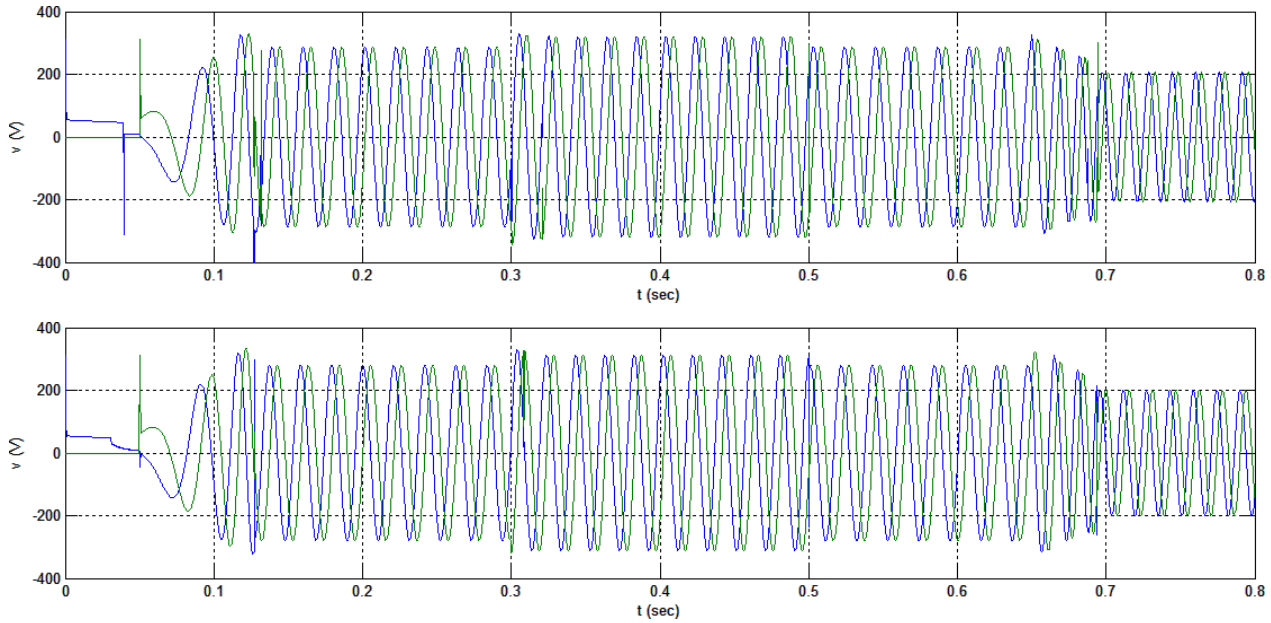

Pic. 5.4-2: Comparison of voltage on stator terminals.

5.4.3 Comparison of stator currents

The last demonstrated waveforms belong to comparison of stator currents. In this case, rotor oriented control achieves lower values. The differences between results are:

- 0,58 *A* during starting of the motor
- 0,1 *A* at no-load state
- 0,13 *A* with nominal load

Again, these differences are not very large, but they would be more significant for larger machines.

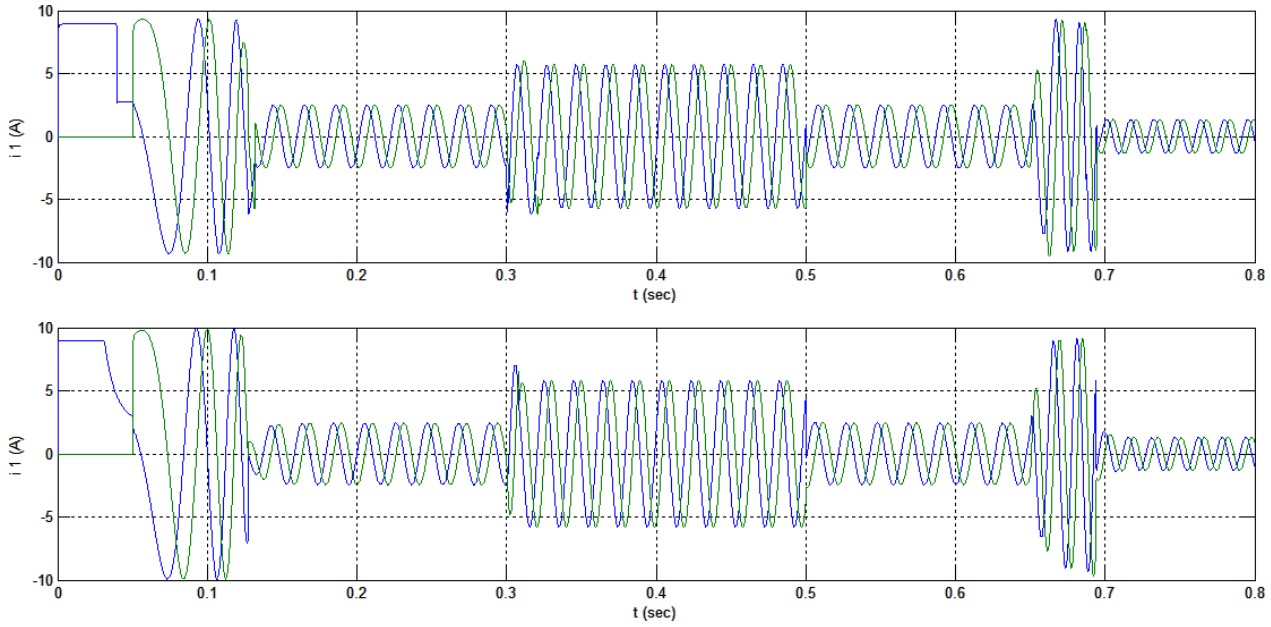

Pic. 5.4-3: Comparison of stator currents.

5.4.4 Conclusion

The result of these three comparisons is that waveforms of couples of parameters were in all cases very similar with only small differences between them. However, it is necessary to mention that the simulations were performed for low power induction machine. For large machines (multiple hundreds or even thousands of kilowatts), the differences would be much greater. Therefore, it is possible to make following conclusion.

As it was mentioned above, both of vector control types are used in general, although rotor oriented control is the mostly preferred type. It might be caused mainly due to lower currents during whole time of operation. Lower currents cause lower power losses (thus decrease in temperatures, as well) in windings of machine according to simple equation (5.4.4-1). This can be specifically essential for long-term operation.

$$P = RI^2 \tag{5.4.4-1}$$

On the other hand, stator oriented vector control is probably preferred in situations, where faster change of speed is needed and lower values of currents are not required. In addition, relations for this type of control are easier to derive.

Finally, it is possible to see that both types of vector control have their advantages and disadvantages one over another. This is the reason why both of them are commonly used. It depends only on requirements of particular application.

6 NATURAL CONTROL OF INDUCTION MACHINE

Last part of this thesis is focused on completely new type of control of induction machine. Author of this type of control is a supervisor of this thesis. This control type was named as natural control because whole algorithm is performed in "natural" reference frame *abc*. There is no need to apply any other reference frames for its realization. Thesis supervisor provided all following mathematical relations mentioned in chapters 6.1 – 6.3.

6.1 Principle of operation

Principle of this control type is illustrated in *Pic. 6.1-1*. The main idea lays in transfiguring series combination of elements L_σ and R/s of equivalent circuit into parallel combination using Γ-network. That ensures presence of equal voltage on all elements of circuit, placed behind resistance of stator winding R_1 what significantly simplifies derivation of relations.

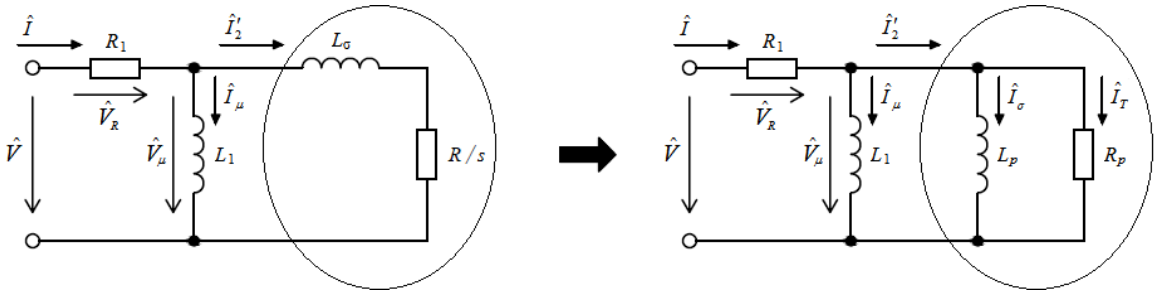

Pic. 6.1-1: Transfiguration of series combination of Γ-network into parallel.

Elements R_p and L_p of transfigured equivalent circuit symbolize so-called parallel resistance and parallel inductance. However, it is necessary to emphasize that these elements do not have constant values. Their values dramatically depend on value of angular velocity ω (on its square) and are defined by relations (6.1-1) and (6.1-2). It is possible to obtain these equations by comparing real and imaginary parts of both impedances.

$$R_p = \frac{R}{s} + \frac{s}{R}\omega^2 L_\sigma^2 \tag{5.1-1}$$

$$L_p = L_\sigma + \left(\frac{R}{s}\right)^2 \frac{1}{\omega^2 L_\sigma} \tag{5.1-2}$$

Reverse calculation of these parallel elements into Γ-network:

$$\frac{R}{s} = R_p \frac{1}{1+\frac{R_p^2}{\omega^2 L_p^2}} \tag{5.1-3}$$

$$L_\sigma = L_p \frac{1}{1+\frac{\omega^2 L_p^2}{R_p^2}} \tag{5.1-4}$$

Although by calculation of these parameters we obtained equal voltage on all elements located behind resistance R_1, transfiguration of equivalent circuit caused division of current I_2' into two fractions I_T and I_σ. Current I_T represents effective value of first harmonic of

torque-producing active component of rotor current I_2' recalculated to stator side. Similarly, current I_σ represents effective value of first harmonic of useless reactive component of rotor current I_2' recalculated to stator side. Magnitude of these currents is defined by relations (6.2-9) and (6.2-10) presented in next subchapter along with final relations for natural control algorithm. By using these relations, a functional model of control has been created in Simulink environment.

6.2 Natural control algorithm

This type of control algorithm certainly does not work on principle of negative feedback. It does work on principle of feed-forward control; meaning that this algorithm calculates all parameters essential for a motor control ahead, while neither speed sensor nor sensor of magnetic flux are used.

Relations for calculating effective value of phase current and voltage:

$$I = \sqrt{\frac{2}{3}[i_A^2(t) + i_B^2(t) + i_A(t)i_B(t)]} \tag{5.2-1}$$

$$V = \sqrt{V_\mu^2 + 2R_1P - R_1^2I^2} = \sqrt{V_\mu^2 + R_1(P + P - R_1I^2)} = \sqrt{V_\mu^2 + R_1(P + P_1)} \tag{5.2-2}$$

where P_1 is an auxiliary parameter; so-called power behind resistance R_1:

$$P_1 = P - R_1I^2 \tag{5.2-3}$$

Relations for calculating active input power of one phase:

$$P = \frac{1}{3}[2v_A(t)i_A(t) + 2v_B(t)i_B(t) + v_A(t)i_B(t) + v_B(t)i_A(t)] \tag{5.2-4}$$

Relation for calculation reference effective value of magnetizing voltage or eventually reference value of magnetic flux:

$$V_\mu = \Psi\omega \tag{5.2-5a}$$

$$\Psi = \frac{V_\mu}{\omega} \tag{5.2-5b}$$

Relation for calculating essential angular velocity of stator rotational magnetic field:

$$\omega = \frac{p_p}{2}\Omega_m(1 - K) + \frac{1}{2}\sqrt{p_p^2\Omega_m^2(1 - K)^2 + 4K\left(p^2\Omega_m^2 + \frac{1}{\tau_R^2}\right)} \tag{5.2-6}$$

where K is second auxiliary constant:

$$K = \frac{P_1\tau_R^2}{(\Psi^2/R) - P_1\tau_R^2} \tag{5.2-7}$$

Ω_m represents a reference value of motor speed in the equation (6.2-6). τ_R^2 represents square of motor time constant - $\tau_R^2 = L_\sigma^2/R^2$.

For a mathematical model of control to be complete, it is necessary to state relations for calculation of following currents, as well:

$$I_T = \frac{P - R_1I^2}{V_\mu} \tag{5.2-8}$$

$$I_\sigma = \sqrt{I^2 - I_T^2} - I_\mu \tag{5.2-9}$$

6.3 Model of control in Simulink environment

In *Pic. 6.3-3*, there is illustrated model of natural control of induction machine created in Simulink environment. In the first moment, this model can appear to be more complicated than model of vector control. By taking, a closer look it is noticeable that most of the blocks are simply created from mutually connected equations (6.2-1) – (6.2-7).

Four necessary filters used for stable functionality of model are labeled with blue color. The block located just behind output from block of equation (6.2-6), labeled as *Limiter*, is highlighted in red. Its function is to prevent reference value of stator rotational magnetic field ω from unexpected deviation more than set range (defined in this block) of reference speed Ω_m. There can be seen inner structure of this block in *Pic. 6.3-1*, and its output characteristic in *Pic. 6.3-2*, where marginal values are highlighted in red. These values must not be overpassed by output. In the case, reference value of angular velocity ω overpasses this range; there would be marginal value in the output instead.

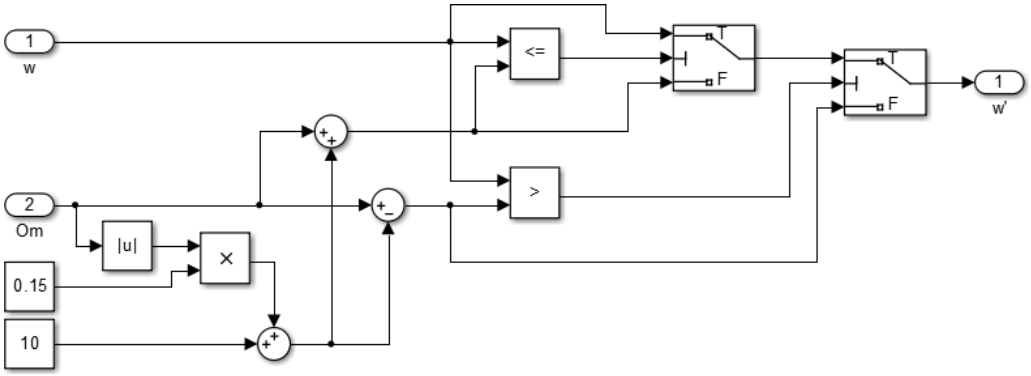

Pic. 6.3-1: Block Limiter.

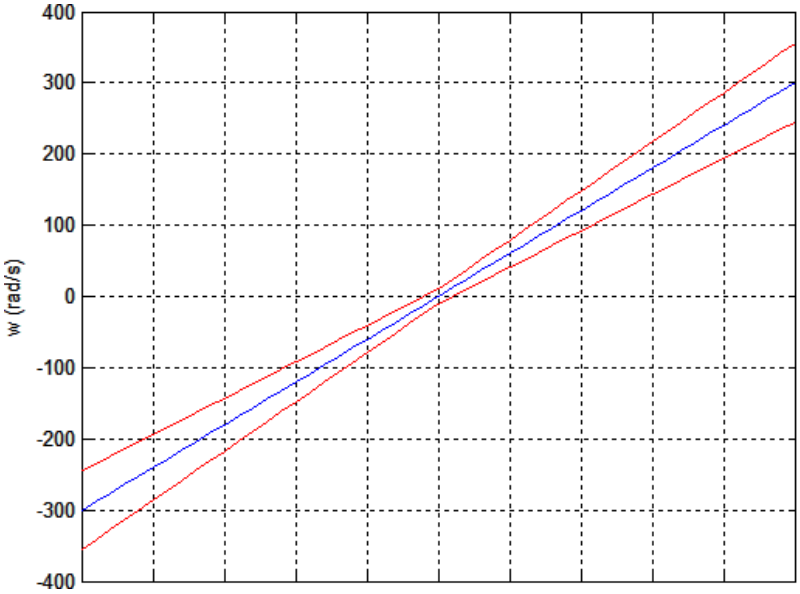

Pic. 6.3-2: Output characteristic of the block Limiter.

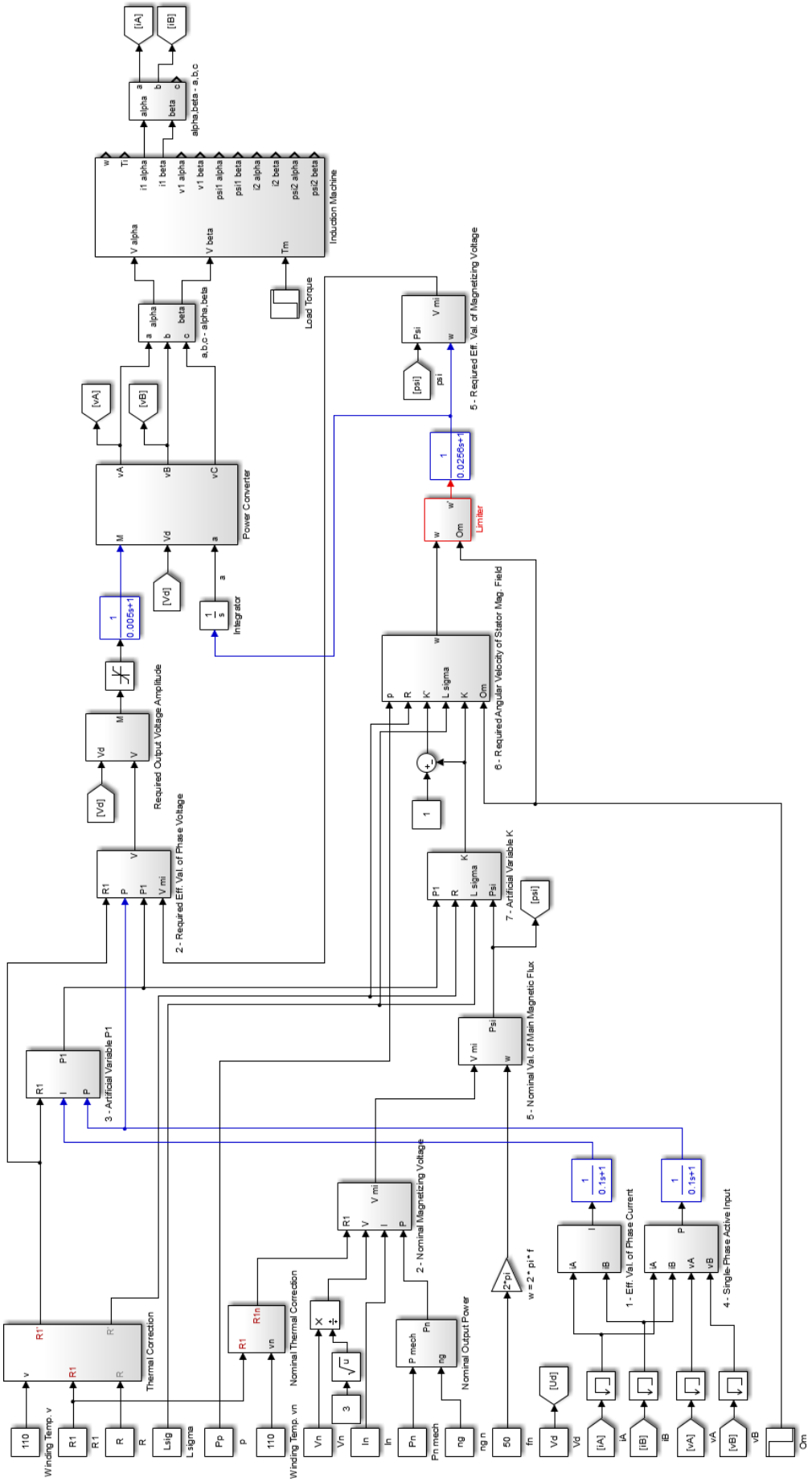

Pic. 6.3-3: Model of natural control created in Simulink environment.

6.3.1 Equation blocks

In this short subchapter, blocks created from relations (6.2-1) – (6.2-7) will be stated together with brief description. In the picture of complete model (*Pic. 6.3-3*), there are block of equations all labeled with numbers 1-7 corresponding with equations.

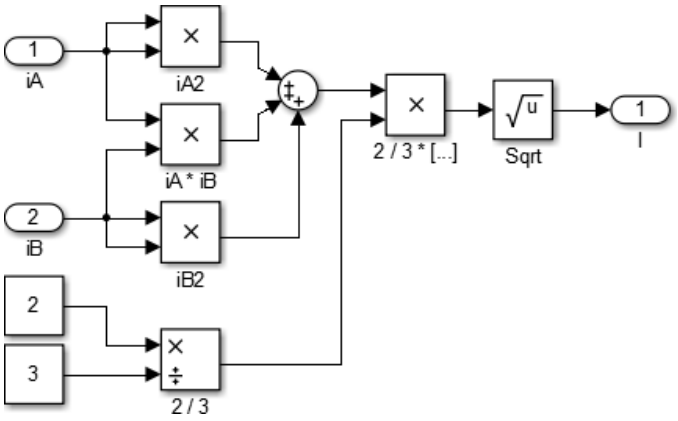

Pic. 6.3-4: Block 1 - calculation of phase current effective value (relation (6.2-1)).

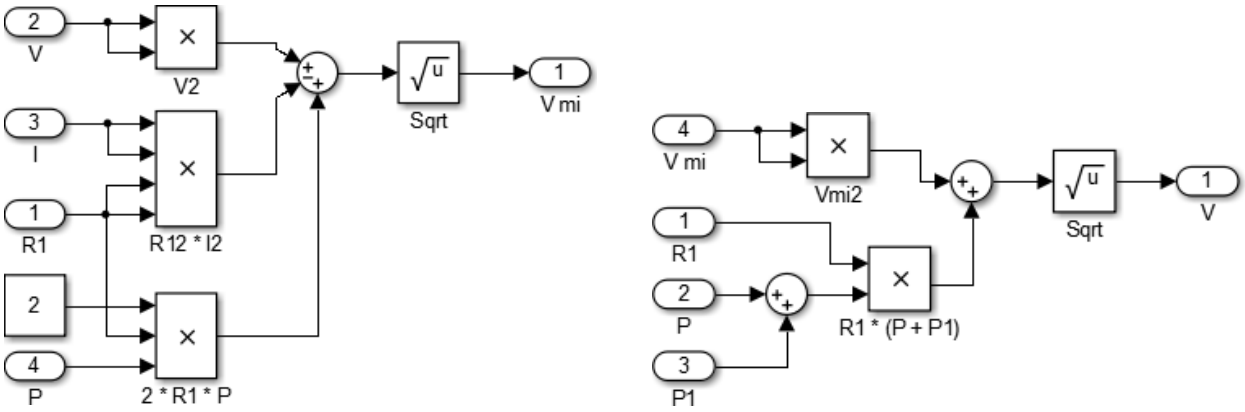

Pic. 6.3-5: Blocks 2 - calculation of effective value of phase voltage or magnetizing volatage, respectively (relation (6.2-2)).

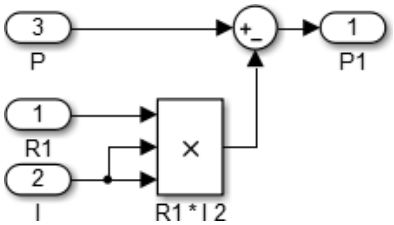

Pic. 6.3-6: Block 3 - calculation of auxiliary variable P_1 (relation (6.2-3)).

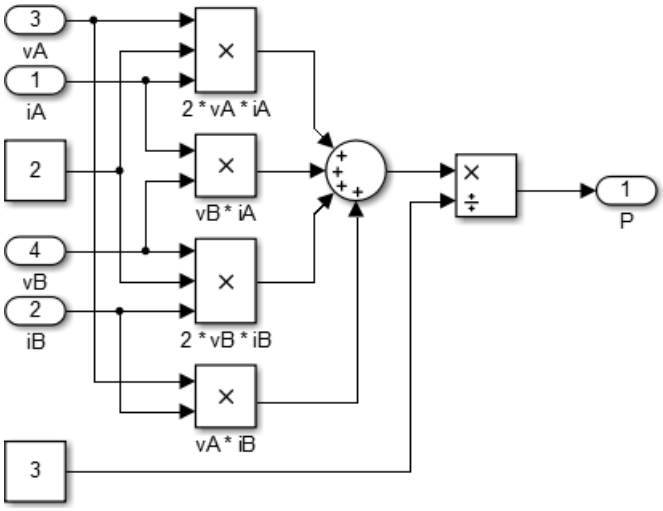

Pic. 6.3-7: Block 4 - calculation of one phase active input power (relation (6.2-4)).

Pic. 6.3-8: Blocks 6 - calculation of reference effective value of magnetizing voltage or reference value of magnetic flux, respectively (relations (6.2-5a), (6.2-5b)).

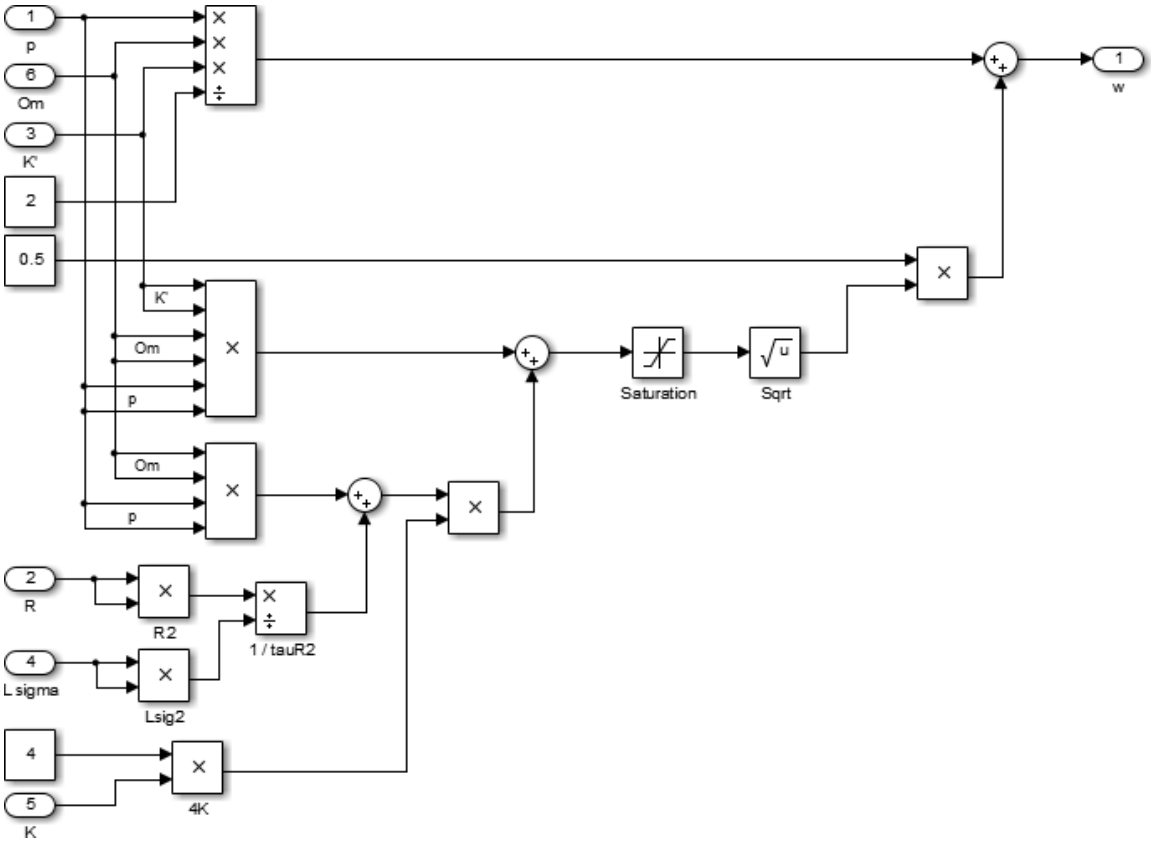

Pic. 6.3-9: Block 6 - calculation of angular velocity of stator magnetic field (relation (6.2-6)).

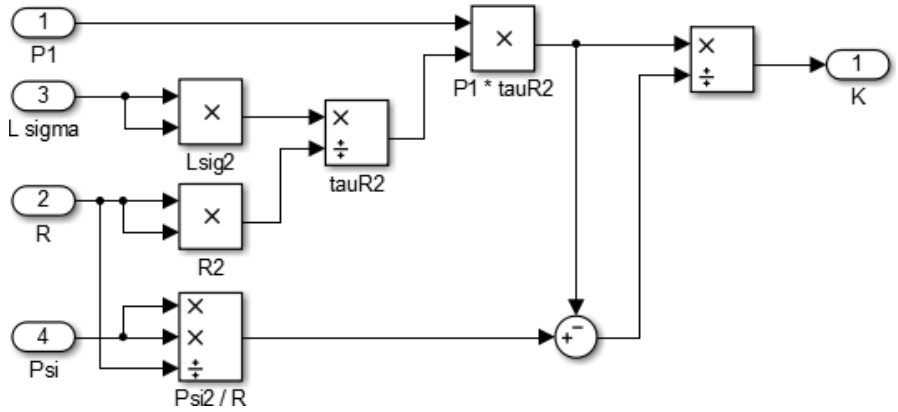

Pic. 6.3-10: Block 7 - calculation of auxiliary constant K (relation (6.2-7)).

6.3.2 Another blocks of model

Model of control shown in *Pic. 5.3-3* contains, besides previously stated blocks, additional five blocks and another block of motor model. This model of motor is also identical with the one used in previous simulations of vector control.

A block for calculating reference value of modulation index is made up from relation (6.3.2-1). Its content is illustrated in *Pic. 5.3.2-1*. Behind this block, there is inserted filter along with saturation block, which defines possible values of modulation index in the range $M \in < 0; 1 >$.

$$M(t) = \sqrt{6}\frac{U(t)}{U_d(t)} \qquad (5.3.2\text{-}1)$$

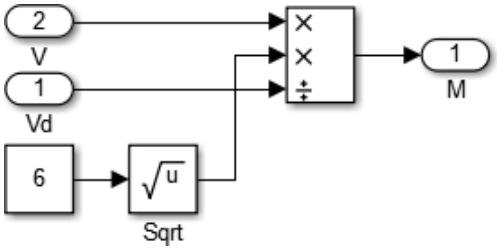

Pic. 6.3-11: Block of modulation index calculation.

The model of motor in this simulation is powered from simple inverter block, whose inner structure can be seen in *Pic. 5.3.2-2*. Three parameters enter a block. First two are value of inverter DC bus voltage V_d and actual value of modulation index, which are used for defining actual amplitude of voltage on stator terminals. Third input parameter is actual magnitude of angle α obtained by integration of angular velocity ω, which is an output out of block *Limiter*. By this angle, sinusoidal signals with amplitude equal 1 are generated. These signals are subsequently multiplied by amplitude of voltage on stator terminals, calculated from first two parameters.

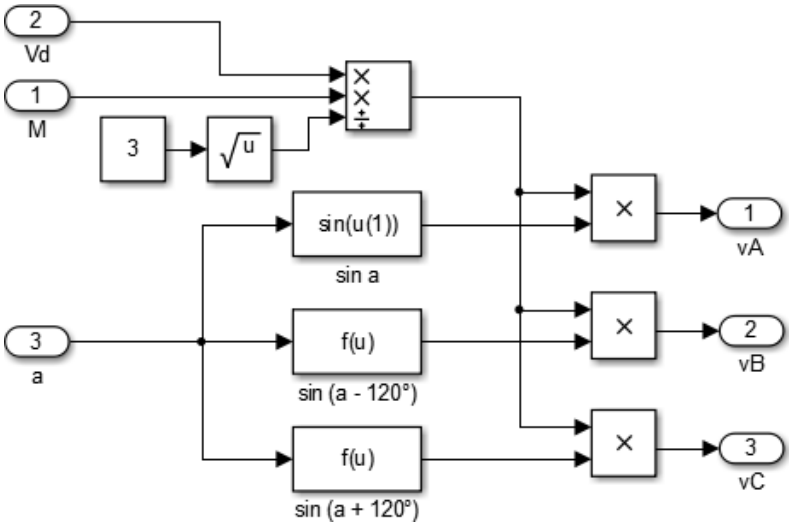

Pic. 6.3-12: Simple model of inverter.

In the model of control, there is further used a calculation of nominal power of the motor. This parameter is calculated using values of nominal mechanical power and motor effectiveness according to relation (6.3.2-2). An inside of the block is illustrated in *Pic. 6.3.2-3*.

$$P_n = \frac{P_{mech}}{3\eta} \tag{5.3.2-2}$$

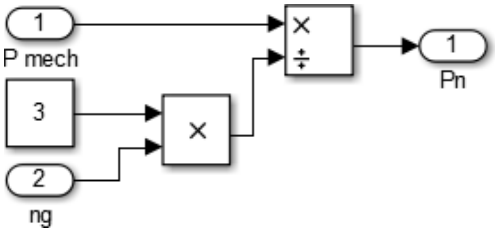

Pic. 6.3-13: Calculation block of motor nominal power.

Last couple of natural control model blocks is blocks of thermal correction, which calculate an effect of temperature on magnitude of resistance. For the calculation, relations (6.3.2-3) for copper material and (6.3.2-4) for aluminum material were used. These equations can be found in literature [1].

$$R_1' = R_1\left(1 + \frac{\vartheta - t_1}{t_1 + 234{,}5}\right) \tag{5.3.2-2}$$

$$R' = R\left(1 + \frac{\vartheta - t_1}{t_1 + 244}\right) \tag{5.3.2-2}$$

where ϑ symbolizes rise of temperature of conductor and t_1 symbolizes room temperature (20 °*C*).

Inner structure of these two blocks is illustrated in *Pic. 6.3.2-4* and *Pic. 6.3.2-5*. Red color symbolizes copper winding and grey symbolizes aluminous squirrel cage of the induction motor.

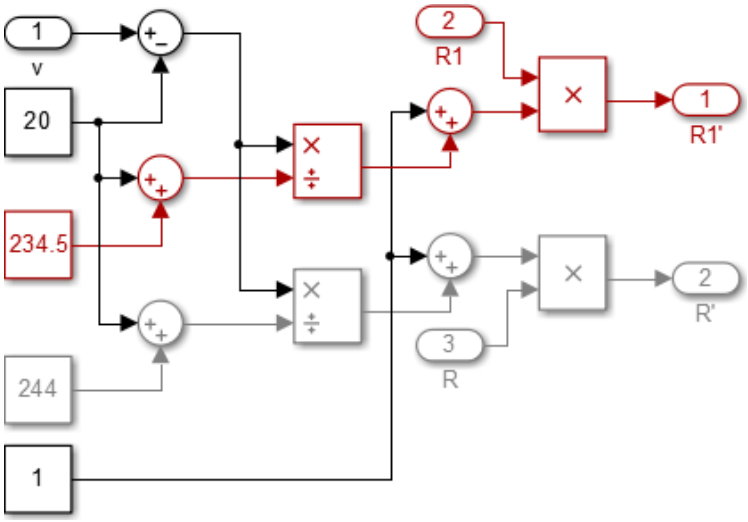

Pic. 6.3-14: Block of thermal correction used for stator winding and squirrel cage.

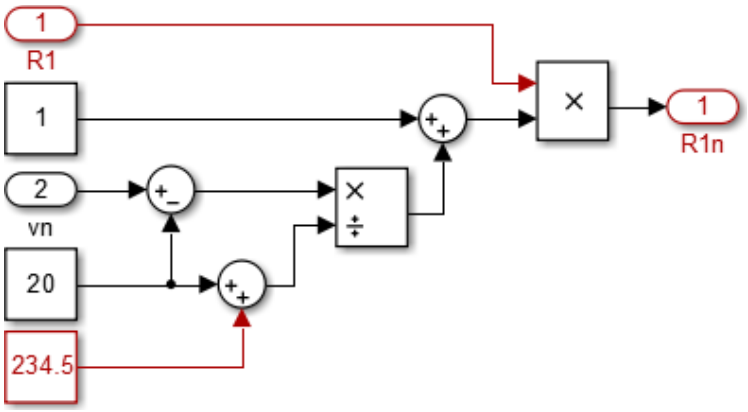

Pic. 6.3-15: Block of thermal correction used for calculation of resistance nominal value.

6.4 Results of simulation

Time waveform of motor angular velocity is illustrated in *Pic. 5.4-1*, where it is possible to see following events. In the first third of waveform the non-loaded motor is starting. Its steady state value of velocity equals exactly to reference value Ω_m = 300 *rad/s*. At time t = 0,55 *s*, nominal load T_L = 7 *Nm* was connected and finally in time t = 1 *s*, reference value of angular velocity decreased from original 300 to 230 *rad/s*.

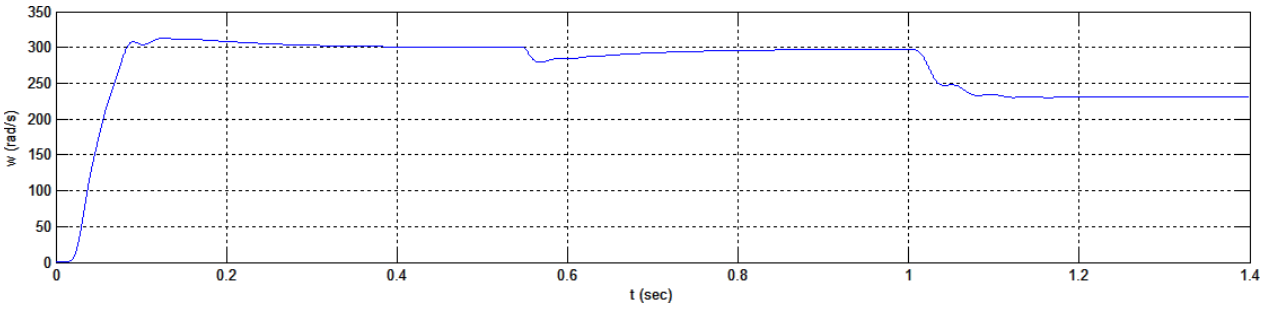

Pic. 6.4-1: Time waveform of motor angular velocity ω.

Steady state value of motor angular velocity after the connection of load is equal 297,5 *rad/s*. This means that magnitude of regulation error is in this case -0,833%. Steady state value of velocity after decrease in reference speed is equal 230,9 *rad/s*. This time, the regulation error has magnitude of +0,391%. Considering that the control model does not contain any speed of flux sensor, but whole regulation is performed using only calculations with use of voltage and current feedback loops of two phases, this are actually good results.

However, using this type of control, during transient events it is not possible to sufficiently control individual parameters of the motor. It is probably caused by use of equations (6.2-1) and (6.2-4). These two equations assume harmonic waveforms of voltages and currents when during transient events this condition is definitely not fulfilled. Insufficient controllability of motor during transient events can be seen in detail of waveforms of phase currents in bottom of *Pic. 6.4-3*. These and also all further waveforms correspond to waveforms in *Pic. 6.4-1*.

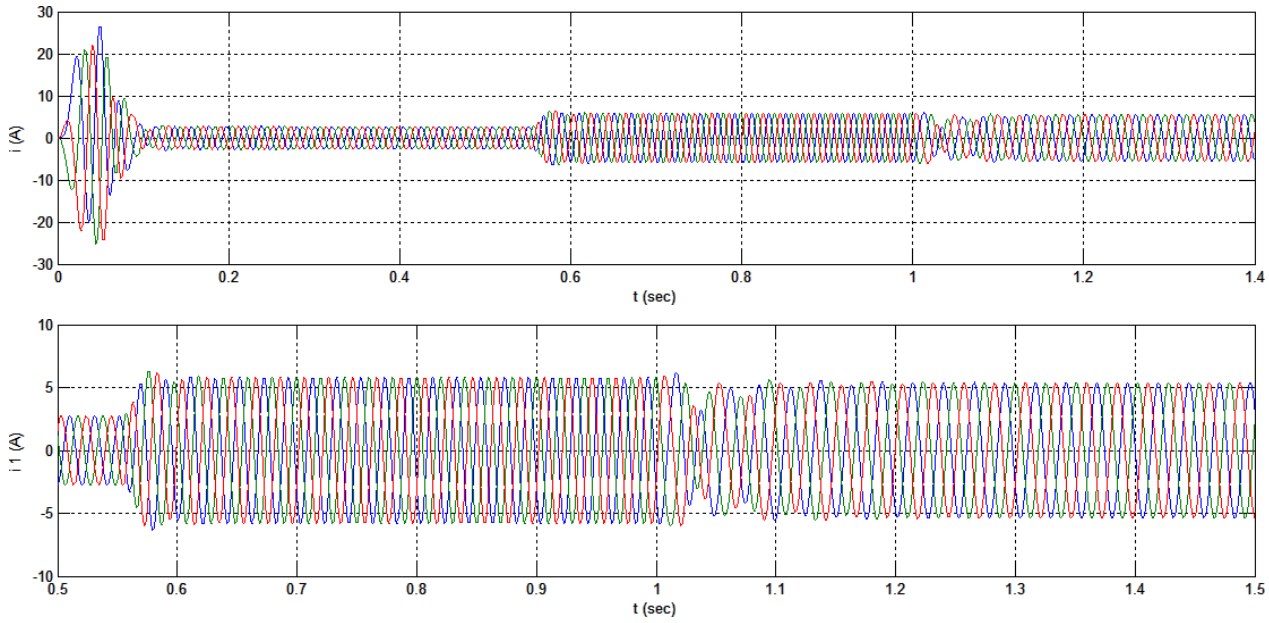

Pic. 6.4-2: Time waveform of stator phase currents i_A, i_B, i_C.

Time waveform of phase voltages on stator terminals and time waveform of modulation index can be found in *Pic. 6.4-3*. Marginal curve (waveform of amplitude) of the voltages is created according to modulation index waveform. It is obvious that during starting of motor and after connection of load, modulation index reaches its maximal value, when the motor is connected to full DC bus voltage of inverter. This limitation of modulation index magnitude has also impact on torque produced by machine. This influence can be seen in *Pic. 6.4-4*, when we can see slight oscillations of torque waveform. Steady state value of torque for non-loaded motor exactly equals zero. This means that mechanical losses (for example friction) were neglected during creation of control model. After connection of nominal load and decrease in speed reference value, the steady state value of torque produced by machine equals 7 *Nm*.

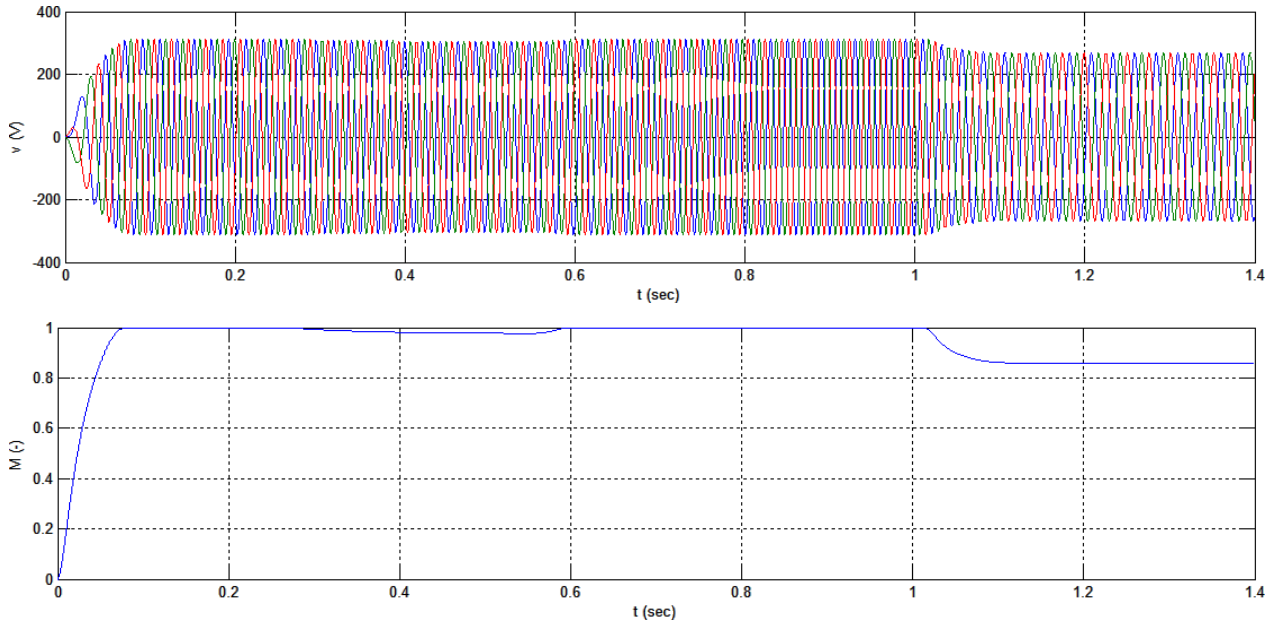

Pic. 6.4-3: Time waveforms of phase voltages on stator terminals and modulation index.

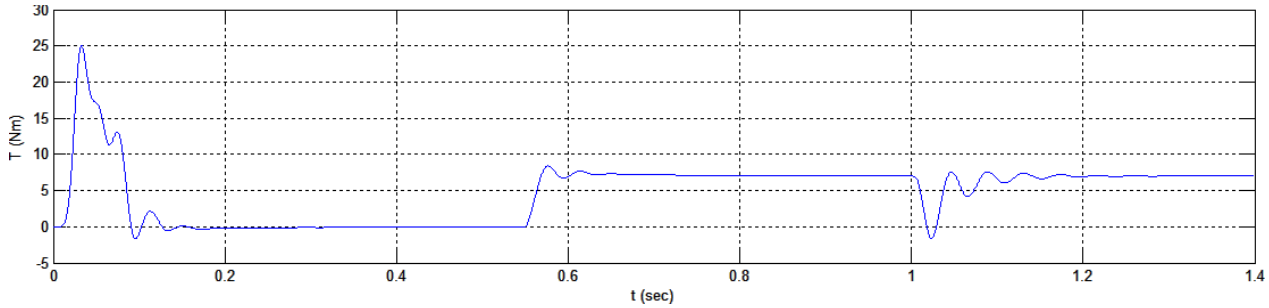

Pic. 6.4-4: Time waveform of torque produced by machine.

Last couple of waveforms belongs to stator and rotor magnetic flux. In these waveforms, we can see that amplitude of both magnetic fluxes moved around value 1 *Wb* during whole time of simulation where amplitude of rotor magnetic flux has always a little lower value than stator flux.

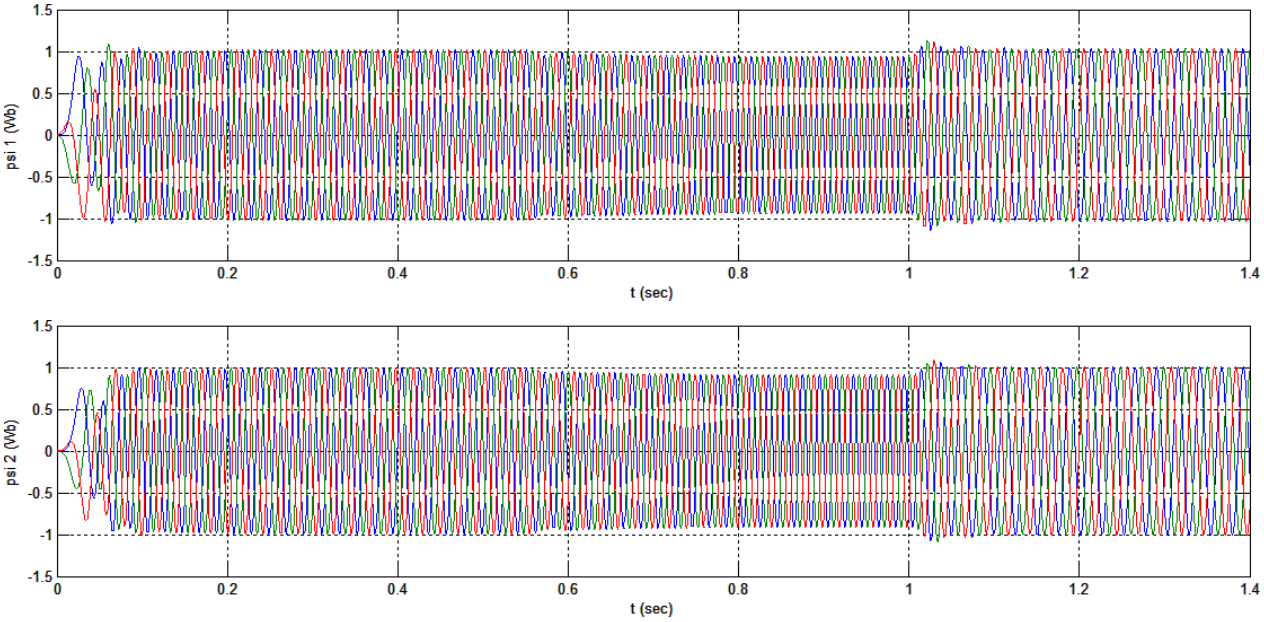

Pic. 6.4-5: Time waveforms of stator and rotor magnetic fluxes ψ_1, ψ_2.

7 CONCLUSION

Content of this thesis can be divided into six main parts. First part is focused on analysis of equivalent circuit configuration variants of the induction machine, specifically equivalent circuit using T-network, Γ-network and Ί-network. This whole chapter is an analogy to the analysis of different equivalent circuit configuration variants of transformer, which can be found in literature [1]. The result is an acknowledgement that configuration variant using T-network is in fact meaningless and unnecessarily complicated, where configuration variant using Γ-network or Ί-network provide multiple advantages in comparison to T-network.

Second part of thesis deals with theoretical analysis of induction machine vector control and derivation of relations for its realization. In conclusion, there was obtained an equation system that can be used for creation of rotor oriented vector control simulation. At the end of second chapter, there is illustrated a block diagram that was further used for realization of control model using Simulink environment.

Third part is dedicated to creation of Simulink model of the induction machine and model of three-phase PWM modulator with inverter. These models were essential for further control simulations. Also, demonstration of functionality of both models was presented just right after explanation of process of construction.

Remaining three parts are focused on simulations of various types of induction machine control – rotor oriented vector control, stator oriented vector control and completely new type of control created by supervisor of this thesis – so-called natural control. It is possible to consider these chapters as a step-by-step guide to creation of each control type from the very beginning. Vector control models contain also not so typical elements, such as de-excitation with user-defined waveform or fully functional PWM modulation. Results for both types of vector control are quite similar and the differences between them are discussed at the end of chapter five. From this, it resulted that each one of them has its advantages and can be used depending on required conditions.

This work also includes the very first attempt of creation functional Simulink model of natural control mentioned above. During this process, it was necessary to include some filters to model in order to achieve satisfying results. Results of simulation are not 100% accurate – there are control deviations with magnitude below 1%. Considering that the control model does not contain any speed of flux sensor, but whole regulation works on principle of feed-forward control, the results are good. However, during transient events it was not possible to sufficiently control individual parameters of the motor. Two used relations that should be probably replaced might be the main reason of these issues.

As stated above, there was performed the first simulation of natural control. Some insufficiencies that could be suppressed in the future were discovered. I would personally recommend further research of this control type as it represents interestingly different approach to the induction machine control.

REFERENCES

[1] PATOČKA, Miroslav: *Magnetické jevy a obvody ve výkonové elektronice, měřicí technice a silnoproudé elektrotechnice*. 1. vyd. Brno: VUTIUM, 2011. 564 s. ISBN 978-80-214-4003-6.

[2] KLÍMA, Bohumil: *Střídavé pohony: učební text*. Brno: VUT, Fakulta elektrotechniky a komunikačních technologií. 98 s.

[3] MĚŘIČKA, Jiří, ZOUBEK, Zdeněk: *Obecná teorie elektrického stroje*. 1. vyd. Praha: SNTL Nakladatelství technické literatury, 1973. 163 s.

[4] PATOČKA, Miroslav: *Vybrané statě z výkonové elektroniky, svazek 2: Pulsní měniče bez transformátoru*. Brno: VUT, 2005. 104 s.

[5] NOVOTNY, D.W., LIPO, T.A.: *Vector Control and Dynamics of AC Drives*. Oxford: Oxford Science Publications, 1996. 464 s. ISBN 0-19-856439-2.

[6] TRZYNADLOWSKI, Andrzej M.: *Control of Induction Motors*. San Diego: Academic Press, 2001. 228 s. ISBN 0-12-701510-8.

[7] TOLIYAT, Hamid A., KLIMAN, Gerald B.: *Handbook of Electric Motors*. 2. vyd. Boca Raton, FL: CRC Press, 2004. 778 s. ISBN 978-0-8247-4105-1.

[8] PISKAČ, Luděk: *Elektrické pohony, principy a funkce*. Plzeň: Západočeská univerzita, 2008, 119 s. ISBN 978-80-7043-688-2.

[9] HRABOVCOVÁ, Valéria, RAFAJDUS, Pavol: *Elektrické stroje, teória a príklady*. 1. vyd. Žilina: EDIS, 2009. 415 s. ISBN 978-80-554-0101-0.

[10] ONDRŮŠEK, Čestmír: *Dynamika elektromechanických soustav: učební text*. Brno: VUT, Fakulta elektrotechniky a komunikačních technologií. 98 s.

[11] HALFAR, L.: *Analýza náhradních zapojení asynchronních motorů*. Brno: VUT, Fakulta elektrotechniky a komunikačních technologií, 2014. 31 s. Vedoucí semestrální práce Ing. Radim Bělošek.

APPENDIX

Parameters used for simulations:

- nominal power of the motor P_n = 2 200 *W*
- nominal stator current I_{1n} = 4,5 *A*
- nominal voltage on stator terminals V_{1n} = 400 *V*
- nominal mechanical angular velocity ω_n = 314 *rad/s*
- number of pairs of poles p_p = 1
- moment of inertia J = 0,0034 kgm^2
- efficiency η = 80,9 %

- inverter DC bus voltage V_d = 540 *V*
- frequency of PWM carrier signal f_{PWM} = 5000 *Hz*

Circuit parameters for Γ-network:

- resistances R_1 = 2,815 Ω R = 2,84 Ω
- main and leakage inductances L_1 = 0,4 *H* L_2 = 0,02 *H*

Parameters R_1, R, L_1, L_2 were also used in form of T-network. They were recalculated according to equations present in literature [11]:

- resistances R_1 = 2,815 Ω R_2 = 3,6286 Ω
- inductances $L_{\sigma 1} = L_{\sigma 2}$ = 0,0096 *H*
  L_h = 0,3904 *H*

For purposes of vector control were inductances of T-network further recalculated. Parameters used for simulations of vector control:

- resistances R_1 = 2,815 Ω R_2 = 3,6286 Ω
- inductances $L_1 = L_2 = L_{\sigma 1} + L_h$ = 0,4 *H*
  L_h = 0,3904 *H*